Resource

Cell Host & Microbe

Identification of Interferon-Stimulated Genes with Antiretroviral Activity

Graphical Abstract

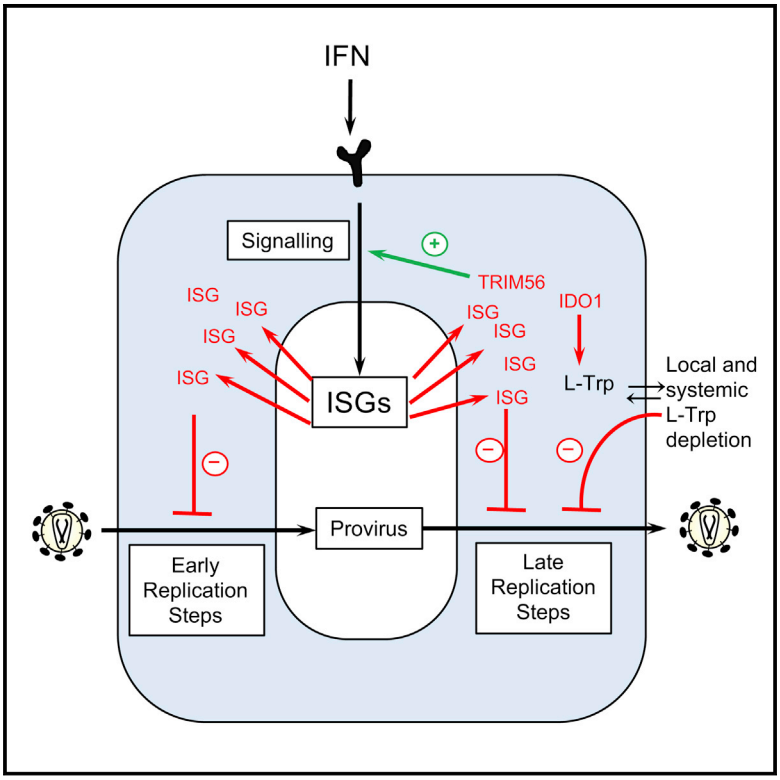

Authors

Melissa Kane, Trinity M. Zang, Suzannah J. Rihn, ..., Charles M. Rice, Sam J. Wilson, Paul D. Bieniasz

Correspondence

sam.wilson@glasgow.ac.uk (S.J.W.), pbienias@adarc.org (P.D.B.)

In Brief

Screening of interferon-stimulated genes for antiretroviral activity reveals numerous genes that directly or indirectly inhibit retroviral replication. Detailed analyses of two antiretroviral effectors indicate that IDO1 inhibits retroviral replication via nutrient depletion while TRIM56 increases the antiretroviral potential of IFNα.

Highlights

- ISG screening identifies direct and indirect antiretroviral proteins
- Interferon-γ inhibits HIV-1 through IDO1-mediated tryptophan depletion
- TRIM56 enhances the antiretroviral potential of interferon-α

Kane et al., 2016, Cell Host & Microbe *20*, 392–405
September 14, 2016
http://dx.doi.org/10.1016/j.chom.2016.08.005

CellPress

Cell Host & Microbe
Resource

Identification of Interferon-Stimulated Genes with Antiretroviral Activity

Melissa Kane,[1,2,7] Trinity M. Zang,[1,2,3,7] Suzannah J. Rihn,[4,7] Fengwen Zhang,[1,2] Tonya Kueck,[1,2] Mudathir Alim,[1,2] John Schoggins,[5] Charles M. Rice,[6] Sam J. Wilson,[4,*] and Paul D. Bieniasz[1,2,3,8,*]
[1]Aaron Diamond AIDS Research Center
[2]Laboratory of Retrovirology
The Rockefeller University, New York, NY 10065, USA
[3]Howard Hughes Medical Institute, Aaron Diamond AIDS Research Center, New York, NY 10016 USA
[4]MRC–University of Glasgow Centre for Virus Research, Institute of Infection, Inflammation and Immunity, University of Glasgow, Glasgow G61 1QH, UK
[5]Department of Microbiology, UT Southwestern Medical Center, Dallas, TX 75390, USA
[6]Laboratory of Virology and Infectious Disease, The Rockefeller University, New York, NY 10065, USA
[7]Co-first author
[8]Lead Author
*Correspondence: sam.wilson@glasgow.ac.uk (S.J.W.), pbienias@adarc.org (P.D.B.)
http://dx.doi.org/10.1016/j.chom.2016.08.005

SUMMARY

Interferons (IFNs) exert their anti-viral effects by inducing the expression of hundreds of IFN-stimulated genes (ISGs). The activity of known ISGs is insufficient to account for the antiretroviral effects of IFN, suggesting that ISGs with antiretroviral activity are yet to be described. We constructed an arrayed library of ISGs from rhesus macaques and tested the ability of hundreds of individual macaque and human ISGs to inhibit early and late replication steps for 11 members of the *retroviridae* from various host species. These screens uncovered numerous ISGs with antiretroviral activity at both the early and late stages of virus replication. Detailed analyses of two antiretroviral ISGs indicate that indoleamine 2,3-dioxygenase 1 (IDO1) can inhibit retroviral replication by metabolite depletion while tripartite motif-56 (TRIM56) accentuates ISG induction by IFNα and inhibits the expression of late HIV-1 genes. Overall, these studies reveal numerous host proteins that mediate the antiretroviral activity of IFNs.

INTRODUCTION

Interferons (IFNs) are a component of an early response to invading pathogens and induce the expression of hundreds of IFN-stimulated genes (ISGs) (Schoggins et al., 2011; Stetson and Medzhitov, 2006). The IFN response can ameliorate viral disease by facilitating clearance of acute infections, or by reducing the volume of chronic virus replication. Additionally, a genetic barrier imposed by species-dependent variation in antiviral ISGs can prevent interspecies transmission of viruses.

Retroviruses are a diverse family that includes human and simian immunodeficiency viruses (HIV and SIV). Multiple observations suggest that IFNs influence retroviral replication, transmission, and pathogenesis. For example, an IFNα antagonist can increase acute SIV replication and accelerate disease progression, while IFNα treatment can prevent SIV infection of macaques (Sandler et al., 2014) and reduce HIV-1 viremia in humans (Asmuth et al., 2010). Moreover, IFN-resistance may be selected during HIV-1 transmission (Fenton-May et al., 2013).

Some proteins with direct antiretroviral activity, such as APOBEC3 proteins, TRIM5α, tetherin, SAMHD1, ZAP, CNP, Mov10, and Mx2 (Doyle et al., 2015; Hatziioannou and Bieniasz, 2011), are encoded by ISGs. Additionally, some ISGs, namely TRIM5 and tetherin, can also exert antiviral effects by signaling to induce other antiviral genes (Galão et al., 2012; Pertel et al., 2011). Thus, response to IFN includes directly antiviral proteins and signal amplifiers that are induced by IFNs (Schoggins et al., 2014; Stetson and Medzhitov, 2006). However, the activity of known ISGs is insufficient to account for the antiretroviral effect of type I IFN, suggesting that some ISGs with antiretroviral activity are yet to be described.

Rapid evolution at host-pathogen interfaces means that ISG evasion or antagonism strategies employed by viruses are often only effective in the native host (reviewed in Doyle et al., 2015). Therefore, antiviral protein activity is sometimes revealed by using viral mutants or non-native viral hosts. HIV-1, for example, evades or antagonizes human APOBEC3, TRIM5α, and tetherin but is fully sensitive to these proteins in non-hominid species (Doyle et al., 2015). Species-dependent variation in antiretroviral proteins can constitute a profound genetic barrier to interspecies retroviral transmission. Accordingly, type I IFN is a significantly more potent inhibitor of HIV-1 and SIV infection in cells of non-native primates (Bitzegeio et al., 2013). Nevertheless, some ISGs exert antiviral effects without evidence for evasion or antagonism by the retroviral target (Doyle et al., 2015).

These concepts shaped our approach to reveal ISGs that inhibit *retroviridae*. We describe an arrayed library of ISGs from a non-human species (*M. mulatta*) and a series of screens in which we tested the ability of hundreds of individual ISGs from humans and macaques to inhibit the replication of eleven

different retroviruses. This approach revealed that IFN's antiretroviral activity is mediated by numerous candidate antiviral factors. We also describe detailed studies of two ISGs (IDO1 and TRIM56) that were revealed by our screens to exhibit antiretroviral activity.

RESULTS

ISG Expression Screening to Identify Genes That Inhibit Retrovirus Replication

We first generated arrayed libraries of hundreds of ISGs in mammalian expression and lentiviral vectors and measured the impact of each ISG on retroviral replication. To expand the utility of a human ISG library (Schoggins et al., 2011) that we previously used to identify pathogen sensors and antiviral effectors (Dittmann et al., 2015; Schoggins et al., 2014; Wilson et al., 2012) and capture the ability of nonhuman ISGs to inhibit retroviruses, we constructed a library of ISGs from rhesus macaques (*M. mulatta*). This arrayed library contained 344 cDNAs from unique macaque ISGs as well as >90 additional ORFs that captured some of the allelic and splicing-generated diversity of macaque ISGs. Together, the two libraries include 488 different ISGs with 252 genes represented by both human and macaque variants (Figure 1A).

To identify human and macaque ISGs with antiretroviral activity, we carried out 25 screens of 11 different retroviruses (Table S1). We conducted these screens in two different ways. First, we used an HIV-1-based lentiviral vector (SCRPSY, Figure 1B) to express each ISG along with TagRFP in target cells that were then challenged with GFP-encoding retroviruses or retroviral vectors. Infection was then measured using two-color flow cytometry. This "incoming screening" strategy (Figure 1C) identifies ISGs that inhibit steps in the retroviral life cycle prior to GFP expression. Second, we co-transfected an ISG-expression plasmid (pDEST40) with a plasmid(s) that generates retroviral particles, then measured the yield of infectious virions by transduction of a GFP reporter gene, or using a reporter cell line. This "production screening" strategy (Figure 1D) identifies genes that inhibit the latter stages of the retroviral life cycle. For each ISG, the fraction of infected, ISG/TagRFP-expressing cells (incoming screens) or the yield of infectious virions (production screens) was expressed as a percentage of the mean value across all wells in a given screen (Figures 1E, 1F, 2A–2G, S1B–S1E, S2, S3, and S4).

Many ISGs Are Capable of Inhibiting Retroviral Replication

The screens identified numerous ISGs that were apparently capable of inhibiting the retroviral life cycle. A number of ISGs that were known to have antiretroviral activity, including several APOBEC3 proteins, TRIM5, tetherin, MOV10, SAMHD1, CNP, and Mx2, were identified in the appropriate incoming or production screens (Figures 1, 2, S1, S2, and S3; Table S5), suggesting that this approach is a powerful way to identify antiviral genes. Many additional ISGs whose expression conferred either resistance to incoming retroviral infection or reduced the production of infectious retroviral particles were identified. Some ISGs appeared to be specific inhibitors of one or a few retroviruses, while others were broadly inhibitory. As examples, OASL inhibited the production of infectious prototypic foamy virus (PFV) virions, and ULK4 inhibited the production of feline immunodeficiency virus (FIV), but OASL and ULK4 had no activity against other retroviruses. Conversely, macaque SLFN12 inhibited the production of all retroviruses (Figures 1, 2, S1, S2, and S3; Table S5). Overall, ~60% of ISGs were hits against a single retrovirus, and the remainder targeted multiple retroviruses. In general, a greater number of ISGs were more potently inhibitory in production screens than in the incoming screens. This finding may result from potentially higher ISG protein levels associated with transient transfection, or may be due to the greater number and complexity of events associated with the late, as opposed to the early, steps of retroviral replication. A number of ISGs appeared to exert antiretroviral activity in a species-dependent manner. For example, human, but not macaque, ANGTPL1 inhibited SIVmac production, while macaque, but not human, IRF2 inhibited HIV-1 infection in human MT4 cells (Figures S1E–S1F and S4; Table S5). More than one-third of the "hits" were identified exclusively using our macaque ISG library (Table S5), but further work is required to determine which of these candidates have genuine species-dependent antiretroviral activity.

The use of lentiviral vectors in incoming screens enabled the effect of ISGs to be determined in different cellular backgrounds. We conducted incoming screens using human CD4+ T cell (MT4) and human CD4+ monocyte (THP-1) cell lines as targets for HIV-1, HIV-2, and SIVmac infection. Interestingly, more ISGs were protective in THP-1 cells than in MT4 cells, even though MT4 cells were more efficiently transduced with the ISG-encoding vectors (Figures 1 and S1; Table S2). Ten ISGs conferred >10-fold protection against infection by at least one primate lentivirus in THP-1 cells but conferred minimal or no protection in MT4 cells (Figures 1, S1, S2, and S3). These genes (cGAS, RIPK2, TLR7, IRF7, TRIM5, TRIM38, MYD88, IL1R, LGALS9, and IFI16) included ISGs known to mediate pattern recognition and inflammatory signaling. Thus, the differential protection conferred by certain ISGs likely reflects the differential ability of THP-1 and MT4 cells to transduce signals.

While ISG screening experiments are a powerful way to identify candidate antiretroviral ISGs, they do not distinguish between genes that act directly on viruses from those that serve a regulatory function. Overexpression screening can also lead to inhibition resulting from unnatural perturbation of cell physiology. ISGs that inhibit one or a few retroviruses are less likely to exert their effects through regulatory or nonspecific mechanisms. However, ISGs with broad activity (e.g., tetherin) can also have important effects. Validation and characterization of all the candidate antiretroviral ISGs identified herein would take many years. We therefore adopted a targeted approach to identify ISGs that (1) act directly to inhibit viral replication or (2) act as regulators of the antiviral state. Importantly, we sought to identify ISGs that affected retrovirus replication at native expression levels.

Some ISGs Inhibit Retroviral Replication by Activating Type I IFN or ISG Expression

To help identify ISGs that inhibited retroviral infection by facilitating the induction of an antiviral state, we determined which

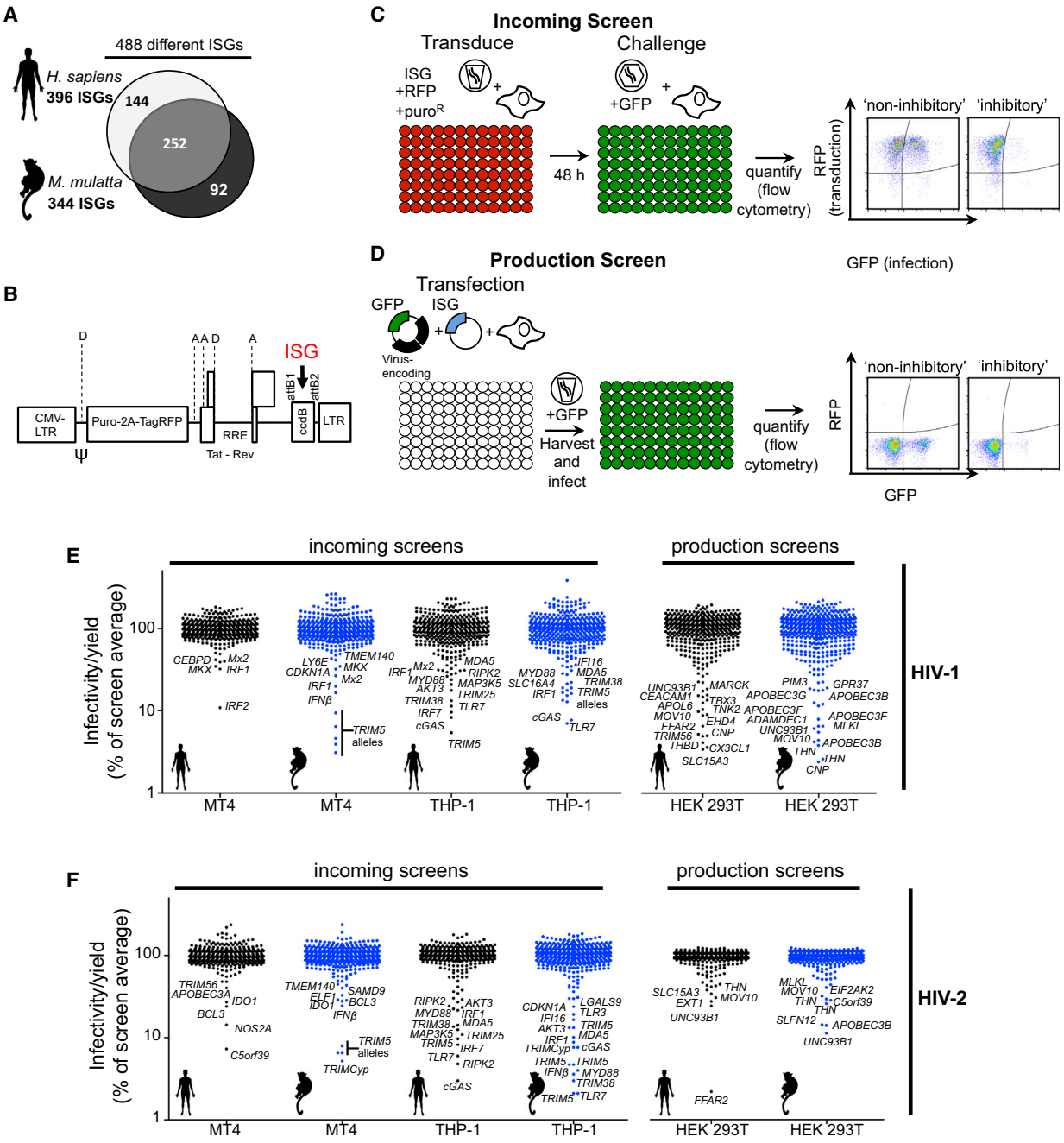

Figure 1. ISG Screening Strategies and Effects of ISGs on HIV-1 and HIV-2

(A) Diagrammatic representations of genes present in the ISG libraries

(B) Schematic representation of the pSCRPSY lentiviral vector. D, splice donor; A, splice acceptor. See Supplemental Experimental Procedures for details.

(C and D) Screening strategy to identify candidate genes that protect cells from incoming retroviral infection (B) or reduce infectious virion yield from infected cells (C).

(E and F) Effect of ISGs in incoming screens with HIV-1 (D) and HIV-2 (E) in MT4 and THP-1 cells and in production screens with HIV-1 (D) and HIV-2 (E) in 293T cells. Black data points, human ISGs; blue data points, macaque ISGs. Hits that appear twice represent variant transcripts. All values were normalized to the screen average (100 a.u.).

ISGs could stimulate expression of type I IFN or other ISGs. We generated 293T and THP-1 cell lines that expressed reporter genes driven by the human IFNβ promoter or an IFN-stimulated response element (ISRE). These cells were transduced with the ISG libraries and reporter gene expression recorded (Figures 3A and 3B; Tables S3 and S4). The ISRE reporter screens were analyzed soon after transduction to minimize potential indirect effects of IFN induction.

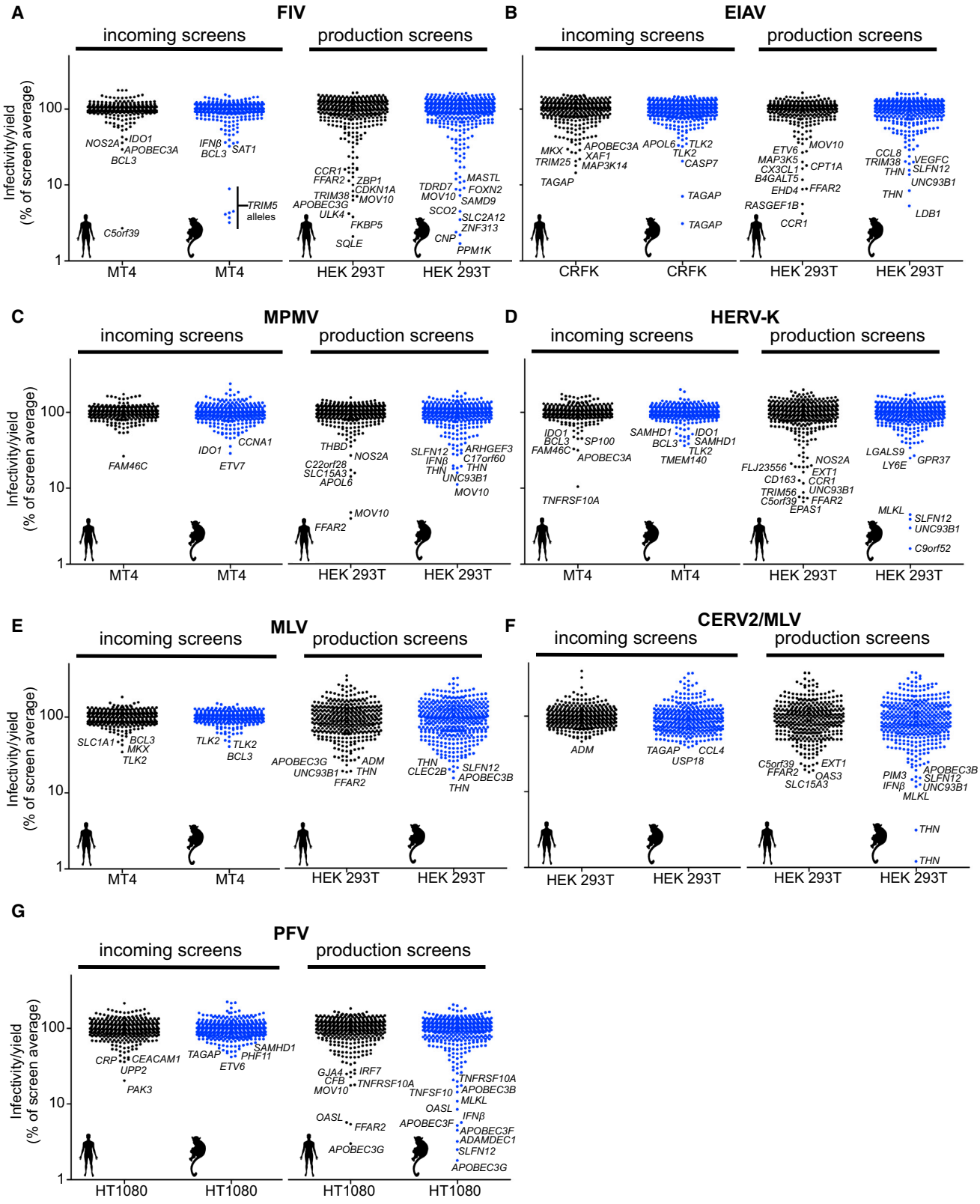

Figure 2. Effects of Human and Macaque ISGs on Diverse Retroviruses

(A–F) The effect of ISGs on lentiviruses, FIV (A) and EIAV (B); betaretroviruses, MPMV (C) and HERV-K (D); gammaretroviruses, MLV (E) and CERV2/MLV (F); and a spumaretrovirus, PFV (G). Screen details are as in Figures 1E and 1F except that the indicated cell lines were used.

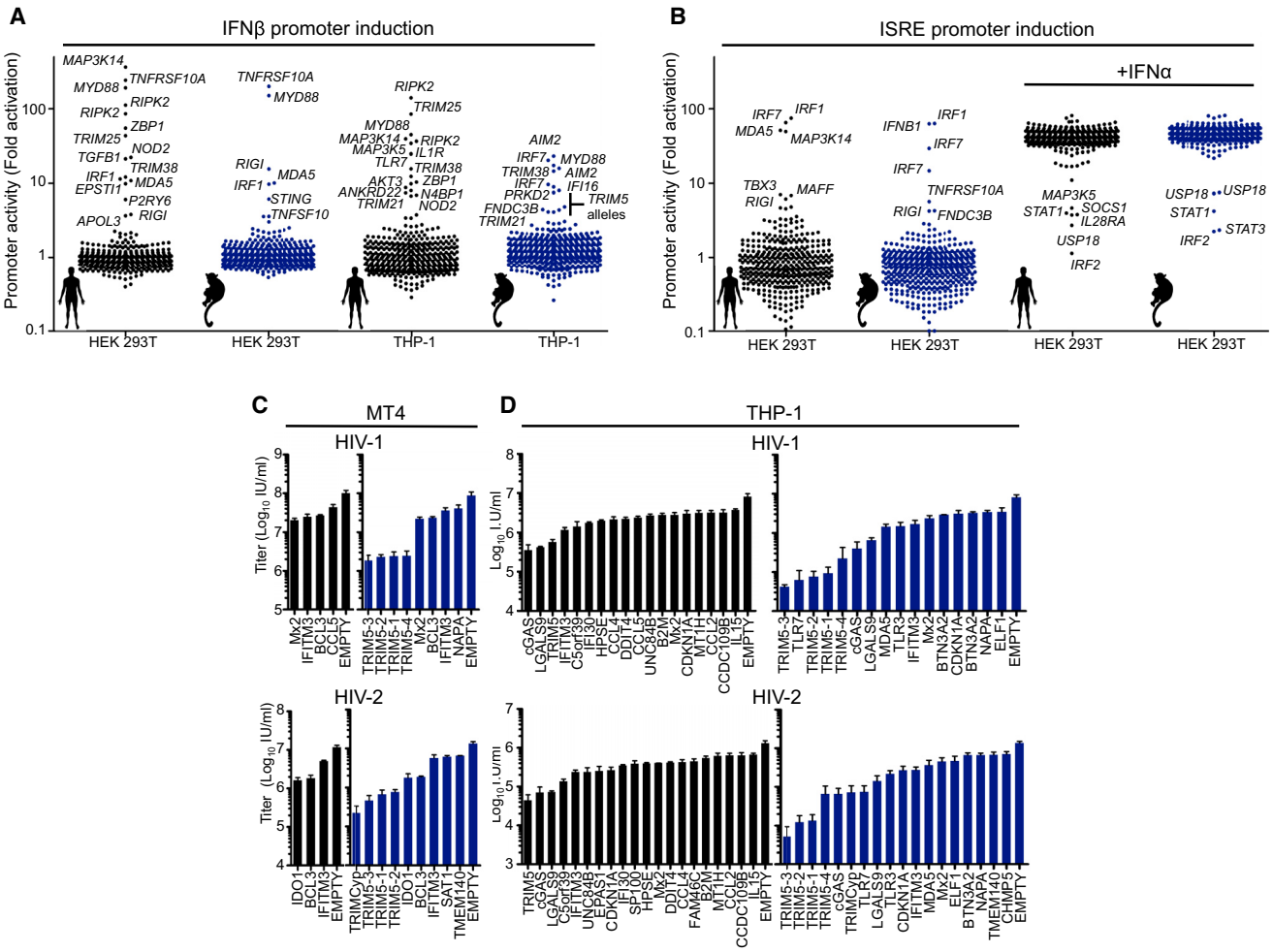

Figure 3. Putatively Indirect and Direct Effects of ISGs on Incoming HIV-1 and HIV-2 Infection

(A) Activation of integrated IFNβ promoter driven luciferase reporter genes in HEK293T and THP-1 cells following transduction with lentiviral vectors encoding macaque and human ISGs.

(B) Activation of integrated ISRE-driven GFP reporter gene in HEK293T cells following transduction with lentiviral vectors encoding macaque and human ISGs.

(C and D) Infectious titers of HIV-1-GFP and HIV-2-GFP in MT4 cells (C) and THP-1 cells (D) transduced with SCRPSY vectors expressing selected ISGs. Titers are mean + SD.

Multiple ISGs that stimulated ISRE or IFNβ promoter activity were identified using this approach. An example was TRIM38, whose expression activated the IFNβ promoter (Figure 3A; Tables S3 and S4). Both human and macaque variants of TRIM38 conferred substantial protection against infection with HIV-1, HIV-2, and SIVmac when expressed in THP-1 cells (5- to 10-fold), but not in MT4 cells (Figures 1, S1, S2, and S3). These findings suggest that TRIM38 may participate in pattern recognition or signaling pathways that lead to type I IFN expression and consequently to inhibition of retroviral infection. As such, this and other proteins identified in this screen are worthy of further investigation as proteins that may regulate IFN expression.

Candidate Directly Acting Inhibitors of Incoming Retroviral Infection

We next elected to pursue ISGs that were likely to directly inhibit incoming HIV-1 or HIV-2 infection. From a list of ISGs that conferred >2-fold protection in any incoming HIV-1 or HIV-2 screen, we selected genes that did not stimulate IFNβ-promoter or ISRE driven reporter expression (Figures 3A and 3B; Tables S3 and S4). Thereafter, we determined infectious titers of HIV-1 and HIV-2 on MT4 and THP-1 cells expressing these ISGs (Figures 3C and 3D). This analysis confirmed the activity of ISGs known to inhibit incoming HIV-1 and HIV-2 infection (such as TRIM5 and Mx2) as well as a number of ISGs for which anti HIV-1 or HIV-2 activity was not previously described (e.g., IDO1, BCL3, LGALS9, and C5orf39) (Figures 3C and 3D). Despite our attempts to focus this sub-screen on directly acting ISGs, several genes that only conferred protection in THP-1 cells, such as cGAS, human TRIM5, and TLRs 3 and 7, likely act by inducing an antiviral state, even though they did not activate IFNβ or ISRE reporters (Figures 3A and 3B). Nevertheless, one ISG that had anti-HIV-1 activity only in THP-1 cells, CDKN1A, may exert its effect by decreasing SAMHD1 phosphorylation (Pauls et al., 2014). Thus, certain ISGs may exert antiretroviral activity, contingent on cofactors that are expressed in a cell-type-dependent manner.

IDO1 Inhibits Retroviral Replication

Of the candidate directly acting, not previously reported, inhibitors of incoming retrovirus infection (Figures 3C and 3D; Table S5), we selected IDO1 for further investigation. IDO1 encodes indoleamine 2,3-dioxygenase 1, which catalyzes the initial rate-limiting step in the conversion of L-tryptophan (L-Trp) to kynurenine (Hayaishi, 1976). Although IDO1 expression is upregulated by type I IFNs, the magnitude of its induction by IFNγ is clearly greater (Hassanain et al., 1993). Notably, IDO1 expression is profoundly upregulated during HIV-1 infection (Favre et al., 2010). IDO1 was active in incoming screens against a number of retroviruses but appeared most potent against HIV-2 (Figures 1F, 2, S1, S2, and S3; Table S5). Interestingly, it reduced both the intensity and the number of EGFP-positive cells (Figures 4A and 4B) and was effective in MT4 cells, but not THP-1 cells (that were less efficiently transduced) (Figure 1).

We generated MT4 cells that inducibly expressed IDO1 (Busnadiego et al., 2014) at levels similar to those in IFNγ-treated A549 cells (in which IFNγ is known to stimulate IDO1 expression) (Figure 4C). In single-cycle infection assays, IDO1 expression in target cells inhibited incoming HIV-2 infection by ~5-fold but did not inhibit HIV-1 infection (Figure 4D). However, in spreading replication assays, IDO1 reduced the number of HIV-1-infected cells by >10-fold for several days (Figure 4E). Correspondingly, the yield of infectious HIV-1 or HIV-2 progeny virions, harvested 44 hr after infection, was reduced by 50- to 100-fold, by IDO1, similar to the reduction conferred by rhTRIM5α over a single replication cycle (Figure 4F). Western blot analyses revealed that IDO1 caused a substantial reduction in HIV-1 Gag, Env, and Nef protein levels, and a corresponding reduction in extracellular particulate CA (Figures 4G and 4H). Thus, IDO1 appears to act by inhibiting viral protein production, and its identification in an incoming screen was the result of reduced reporter gene expression.

IDO1-driven generation of kynurenine can have immune regulatory effects (Opitz et al., 2011) and deplete L-Trp (Pfefferkorn, 1984; Schmidt and Schultze, 2014). Single-cycle HIV-1 replication was inhibited when cells MT4 expressing inducible IDO1 were mixed with unmodified cells, even when <50% cells expressed IDO1 (Figure 4I). This finding suggested that IDO1 inhibits HIV-1 through L-Trp catabolites or by L-Trp depletion, rather than the direct action of the IDO1 protein. Moreover, 1-methyl-L-tryptophan (1-MT), a competitive inhibitor of IDO1 enzymatic activity, substantially reversed the anti-HIV-1 effect of IDO1 (Figure 4J). Crucially, L-Trp supplementation fully restored IDO1-inhibited HIV-1 Gag expression and infectious particle generation (Figure 4K). In the absence of IDO1, treatment with 1-MT or additional L-Trp had little influence on infectious progeny virion yield (Figure S5A and S5B). Because L-Trp supplementation should not prevent the formation of IDO1-specific catabolites, IDO1 appears to inhibit HIV-1 through L-Trp depletion.

IDO1 Can Constitute a Major Component of IFNγ-Mediated Inhibition of HIV-1

We next considered whether endogenous IDO1 contributes to the anti-HIV-1 activity of IFNγ (Hammer et al., 1986). IDO1 is induced in antigen-presenting cells (APCs) following HIV-1 infection in vivo or IFNγ stimulation in vitro (Favre et al., 2010), but most immortalized cell lines do not respond to IFNγ in this way. Therefore, we used A549 cells, which, unusually, exhibit robust IDO1 induction following IFNγ treatment (Figure 5A). IFNγ treatment of A549 cells conferred only 2- to 3-fold protection from incoming pseudotyped HIV-1 infection (Figure 5B). In contrast, IFNγ caused up to 100-fold reduction in HIV-1 infectious virion yield from infected A549 cells in a single cycle of replication (Figure 5C). Addition of L-Trp or 1-MT increased the yield of infectious HIV-1 from IFNγ-treated A549 cells by ~10-fold (Figure 5D) but did not have this effect in the absence of IFNγ (Figure S4C). A similar L-Trp induced rescue of infectious virion yield occurred with IFNγ–treated TZM-bl cells, a commonly used HIV-1 indicator cell line (Figures 5D–5F and S5D). Thus, IDO1-induced nutrient (L-Trp) depletion is responsible for a substantial fraction of the anti-HIV-1 activity of IFNγ in A549 and TZM-bl cells.

TRIM56 Expression Inhibits HIV-1 Replication

As an alternative approach to identify ISGs that could mediate the antiretroviral activity of IFNα, several genes that were hits in outgoing HIV-1 screens (>3-fold inhibition) were tested for their ability to inhibit spreading HIV-1 replication when stably expressed in GHOSTX4 indicator cells. HIV-1 replication in GHOSTX4 cells is resistant to inhibition by IFNα (our unpublished data), so this strategy could, in principle, capture ISGs that regulate the antiviral state, or directly inhibit late HIV-1 replication steps. Most of the selected ISGs modestly inhibited HIV-1 replication GHOSTX4 cells (Figures 6A and 6B), but one ISG, TRIM56, substantially delayed HIV-1 spread (Figure 6A). TRIM56 has previously been reported to inhibit the replication of some, but not all, RNA viruses through mechanisms that are unclear (Liu et al., 2014; Wang et al., 2011). In our screens, TRIM56 greatly inhibited the production of infectious HIV-1 and HERV-K virions and exhibited weak activity against HIV-2 in incoming screens (Figures 1E, 1F, and 2D).

We confirmed the apparent specificity of the effect of TRIM56 by cotransfecting varying amounts of TRIM56 expression plasmid with plasmids generating infectious HIV-1 or MLV particles. TRIM56 reduced the yield of infectious HIV-1 particles by up to 50-fold (Figures S6A and S6B) but had little effect on MLV particle yield (Figures S6C and S6D). Western blot analysis revealed that TRIM56 reduced the levels of cell- and virion-associated HIV-1 Gag but did not affect MLV Gag expression. Thus, exogenous TRIM56 appeared to specifically inhibit HIV-1 gene expression.

We next generated nine single-cell clones of GHOSTX4 cells expressing TRIM56 at levels that were only modestly higher than unmodified GHOSTX4 cells (Figure 6C) and significantly lower than the transiently transfected 293T cells used in the cotransfection and screening experiments (Figures S6A and S6C). When the GHOSTX4-TRIM56 clones were challenged with HIV-1, viral spread was significantly delayed (four clones) or apparently abolished (five clones; Figures 6D and 6E). Despite this dramatic inhibition of viral spread, approximately equivalent numbers of control and TRIM56-expressing cells were infected in the initial infection cycle (Figure 6D). This finding is consistent with the notion that TRIM56 inhibits late rather than early steps of HIV-1 replication (Figure 1E).

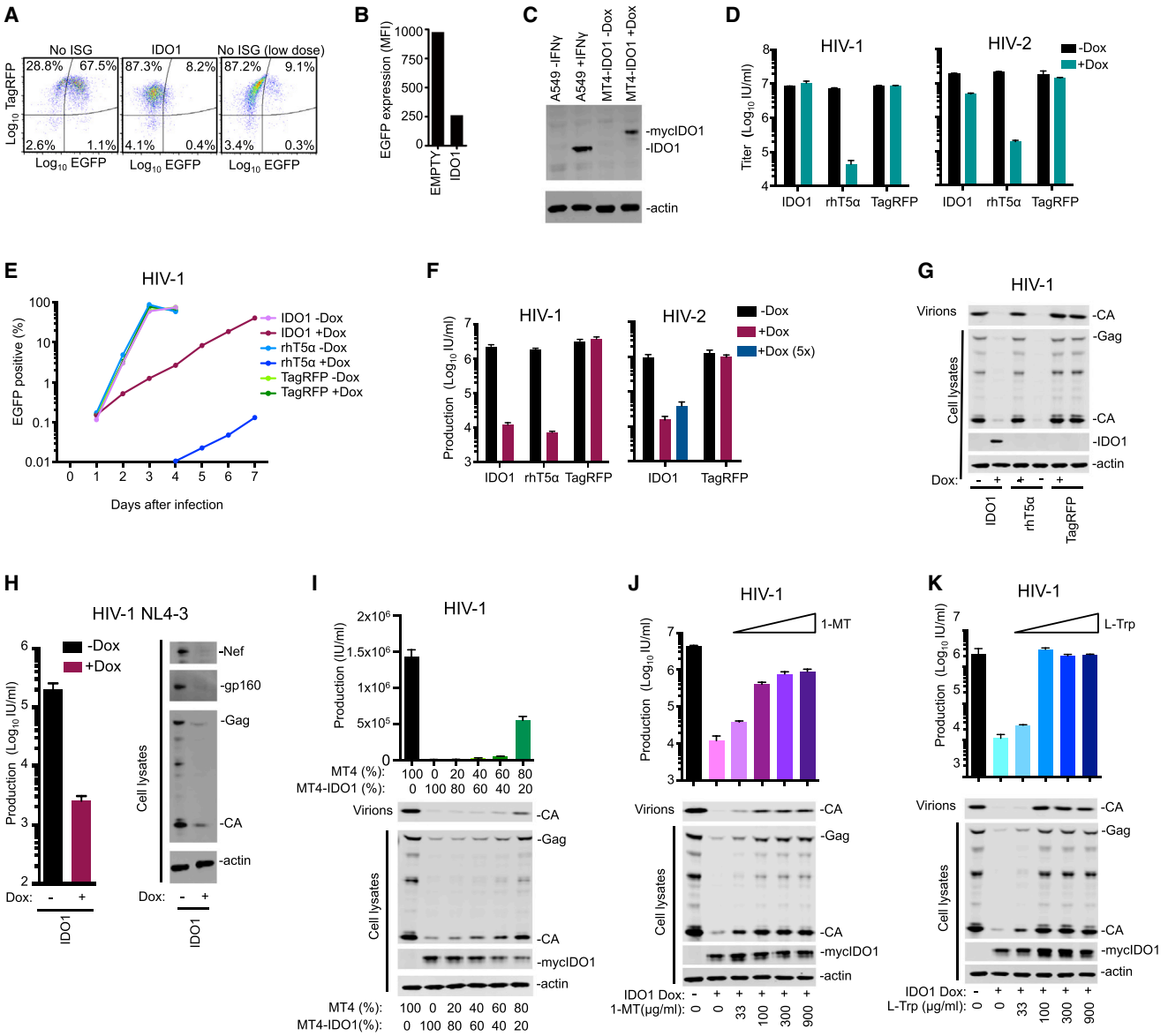

Figure 4. IDO1 Inhibits HIV-1 and HIV-2 Replication

(A and B) FACS plots (A) and quantitation of mean fluorescence intensity (MFI, B) depicting GFP expression following standard or low-dose HIV-2-GFP infection of MT4 cells transduced with vectors expressing no ISG or IDO1.

(C) Western blot (WB) analysis of IDO1 expression with or without induction by IFNγ (A549 cells) or doxycycline (Dox) (MT4-IDO1 cells).

(D) Infectious titer of HIV-1-GFP (NHG) or HIV-2-GFP in target MT4 cells containing Dox-inducible IDO1, rhT5α, or TagRFP.

(E) HIV-1-GFP (NHG) replication in MT4 cells containing Dox inducible IDO1, rhesus TRIM5α (rhT5α), or TagRFP.

(F) Production of infectious HIV-1-GFP (NHG) or HIV-2 (VSV-G pseudotyped ROD10) during a single cycle of replication in MT4 cells containing Dox inducible IDO1, rhT5α, or TagRFP. Where indicated (5×), 5-fold higher input was used to negate the "incoming" effect.

(G) WB analysis of Gag expression in the same HIV-1 (NHG) infected cells as in (F).

(H) Infectious titer of HIV-1 produced and WB analysis of Gag, Env, and Nef expression in MT4 cells containing Dox-inducible IDO1 during a single cycle of HIV-1 (NL4.3) replication.

(I) Yield of infectious virions and cell lysate and particulate capsid during a single replication cycle of mixed (in the indicated ratios) unmodified MT4 cells and MT4 cells containing Dox-inducible IDO1.

(J and K) Effects of 1-MT (J) or L-Trp (K) on the yield of infectious HIV-1 particles and WB analysis of expression and release of viral Gag proteins during a single cycle of HIV-1 replication in MT4 cells containing Dox-inducible IDO1. Titers are mean + SD.

Western blot analysis of a single cycle of HIV-1 replication in one GHOSTX4-TRIM56 cell clone (#2) revealed that the product of an early HIV-1 gene (Nef) was not affected by TRIM56 (Figure 6F). Conversely, Gag and Env expression and the yield of viral particles were significantly reduced in GHOSTX4-TRIM56#2 cells (Figure 6F). The reduction in yield of HIV-1

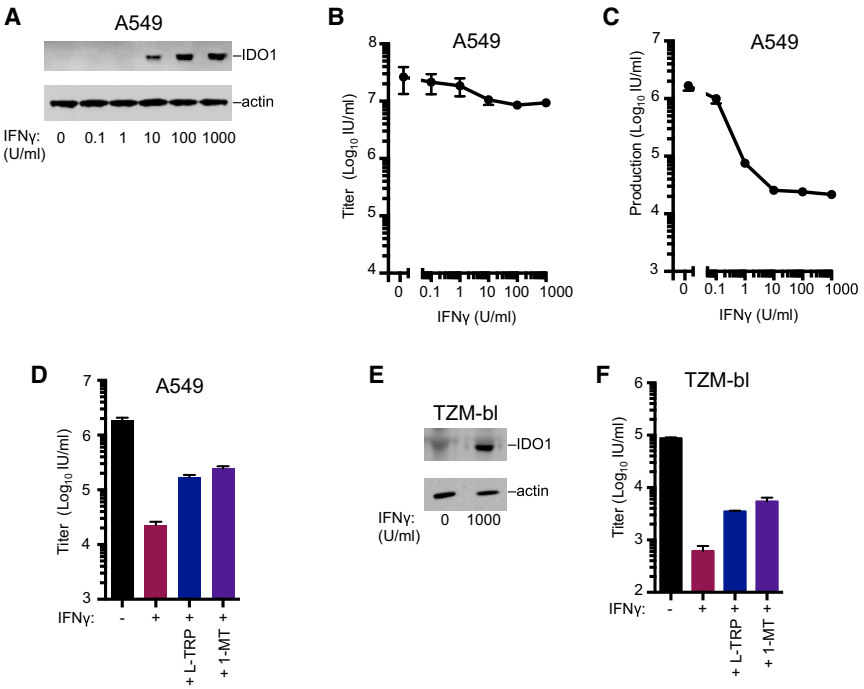

Figure 5. Endogenous IDO1 Inhibits HIV-1

(A) WB analysis of IDO1 expression in IFNγ-treated A549 cells.

(B) Titer of VSV-G pseudotyped replication competent HIV-1-GFP (NHG) on A549 cells following treatment with increasing doses of IFNγ.

(C) The yield of infectious progeny virions from a single cycle of HIV-1 replication in A549 cells treated with increasing doses of IFNγ.

(D) The yield of infectious progeny virions from a single cycle of HIV-1 replication in A549 cells treated with IFNγ in the presence of 50 μg/ml L-Trp (D and E) or 100 μg/ml 1-MT (D and F).

(E) WB analysis of IDO1 expression in IFNγ-treated TZM-bl cells.

(F) As in D using TZM-bl cells. Titers are mean + SD.

particles as measured by quantitative western blotting or using infectivity assays was similar (Figures 6G and S6E), indicating that TRIM56 reduced the number but not the infectiousness of virions generated by infected cells.

TRIM56-Induced Inhibition of HIV-1 Involves Multiple Viral and Host Genes

To identify viral determinants of TRIM56 sensitivity, we passaged HIV-1 in GHOSTX4-TRIM56 cells. Replication was eventually detected in some GHOST-TRIM56 clones (Figure 6E), and virions harvested from these cells were used to initiate an iterative passage series in GHOSTX4-TRIM56#2 cells (Figure 6H). After eight passages, replication was only modestly delayed in GHOSTX4-TRIM56#2 cells. Sequence analysis of a full-length molecular clone of the adapted virus (termed HIV-1/TRIM56R) revealed numerous mutations including a frameshift in Vif and missense mutations in Gag, Pol, Vpr, Tat, Rev, and Env (Figure 6I). In single-cycle replication experiments, the yield of WT HIV-1 virions was diminished in the TRIM56-expressing clones, while HIV-1/TRIM56R yielded similar levels of virions from control and TRIM56-expressing cells (Figure 6J).

Unlike WT HIV-1, the cloned HIV-1/TRIM56R virus replicated robustly in GHOSTX4-TRIM56#2 cells (Figure 7A) and with slightly faster kinetics than WT HIV-1 in unmodified GHOSTX4 cells. Analysis of chimeric proviruses containing either the 5′ or 3′ half of the HIV-1/TRIM56R genome (5′R and 3′R; Figure 6I) suggested that TRIM56 resistance mapped to the 3′R region (Figure 7B). Further analysis of chimeric viruses containing elements from 3′R indicated that the TRIM56 resistant phenotype could not be mapped to a single determinant (our unpublished data). Nevertheless, a single substitution in the HIV-1 Env gene (T6421A, Env N67K) present in 3′R enabled some level of replication in GHOSTX4-TRIM56 cells (Figure 7B). When the T6421A mutation was combined with mutations in 5′R (generating HIV-1 5′R-6421), the HIV-1/TRIM56R virus phenotype was reproduced. Attempts to map determinants within 5′R conferring TRIM56 resistance upon HIV-1 5′R-6421 again indicated that multiple determinants in 5′R contributed to the HIV-1/TRIM56R phenotype (our unpublished data). Thus, the ability of the HIV-1/TRIM56R virus to replicate in GHOSTX4-TRIM56#2 cells was conferred by the cumulative effect of multiple mutations and not governed by a single viral gene.

To determine whether endogenous TRIM56 could inhibit HIV-1 replication, we used CRISPR editing to disrupt *TRIM56* in an MT4 cell clone that contains an HIV-1 LTR-driven GFP gene (MT4/LTR-GFP). We generated four Cas9-expressing MT4/LTR-GFP subclones in which *TRIM56* was not perturbed, and seven expressing Cas9 and *TRIM56*-targeted guide RNAs. All control MT4/LTR-GFP clones expressed equivalent levels of TRIM56, while the *TRIM56* targeted clones expressed greatly reduced or undetectable levels of TRIM56 (Figure 7C). HIV-1 replicated with nearly identical kinetics in each of the cell clones (Figure 7D), indicating that they were equally permissive and that endogenous TRIM56 does not inhibit HIV-1 replication (Figure 7D). Strikingly, however, in the presence of IFNα, which elevated the level of TRIM56 expression ~2-fold (Figures S7A and S7B), replication was inhibited to a far greater extent in unedited clones compared to clones in which *TRIM56* was disrupted.

Because resistance to TRIM56 involved multiple viral genes, and the antiviral effect of endogenous TRIM56 was evident only upon IFNα treatment, it was possible that TRIM56 acted by increasing the levels or effects of other antiviral proteins. A microarray analysis of the four control and sevevn *TRIM56* knockout MT4 clones, focusing on the 120 most highly IFNα-induced ISGs, revealed that, despite variation among individual cell clones, basal ISG expression (i.e., in the absence of IFN) was generally unaffected by TRIM56 (Figure 7F). In contrast, following IFNα treatment, many ISGs were expressed at higher levels in control than in *TRIM56* knockout clones (Figure 7G). These genes included several that were hits in our screens (Figure 1C), as well as known antiretroviral genes, including APOBEC3G, Mx2, MOV10, and IFITM3. Analysis of a larger set

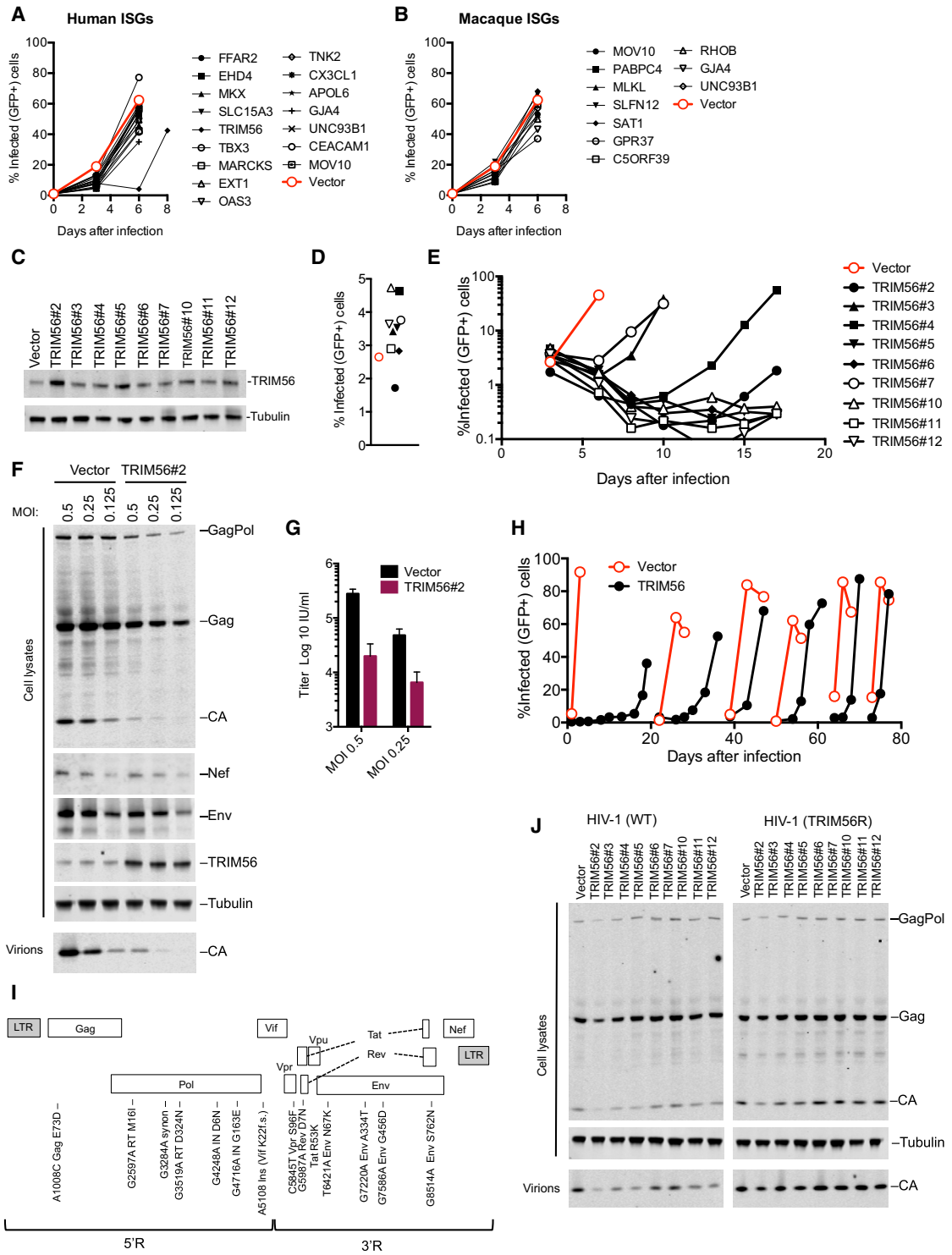

Figure 6. TRIM56 Overexpression Can Inhibit HIV-1 Replication

(A and B) HIV-1 replication in populations of GHOST cells transduced with lentiviral vectors (CCIB) expressing the indicated human (A) or macaque (B) ISGs.

(C) WB analysis of GHOST cell clones overexpressing TRIM56.

(D) Single round HIV-1 infection of GHOST cells transduced with empty vector (CCIB, filled symbol) or clones overexpressing TRIM56.

(E) Spreading replication of HIV-1 in GHOST cells transduced with empty vector (CCIB, red symbol) or the clones overexpressing TRIM56 described in (C).

(F) WB analysis of Gag, Nef, Env, and TRIM56 expression and particle release in GHOST vector and GHOST-TRIM56#2 cells during a single cycle of HIV-1 infection.

(G) The yield of infectious progeny virions from a single cycle of HIV-1 replication in GHOST-vector and GHOST-TRIM56#2 cells.

(legend continued on next page)

of 500 ISGs (Figures S7C and S7D) confirmed that *TRIM56* knockout reduced ISG expression following IFNα treatment. Thus, TRIM56 likely enhances the antiretroviral activity of IFNα, at least in part, by enhancing cellular responsiveness to this cytokine.

DISCUSSION

Here we report the most comprehensive screen of ISGs yet undertaken for antiviral activity against a given virus family. Previously, we conducted a narrowly focused incoming screen that tested the ability of human ISGs to inhibit HIV-1 (Schoggins et al., 2011). Notably, those results are generally consistent with this study, with five of seven ISGs re-identified in this study. However, in this study we identified many additional candidate anti-retroviral genes, a large number of which have not previously been reported to have antiretroviral activity. In general, our findings underscore the complexity of the interferon response with respect to inhibition of retroviral replication and suggest that the antiretroviral activity of type I IFN is mediated and regulated through the action of many ISGs (Table S5). Some ISGs appeared to act in a retrovirus-specific manner, while others had broad activity (Table S5). We also found some discrepancies in the antiretroviral activity between human and macaque variants of ISGs, which may contribute to the species-dependent barriers to retroviral replication that can be erected by type I IFN treatment (Bitzegeio et al., 2013). However, a caveat is that the screens were conducted in human cells, and it is possible that some ISGs may only function properly in cells of species from which they originate. Clearly, some of the genes identified herein act to enhance or modify signaling pathway rather than as directly antiviral proteins, while others appear to have direct antiviral activity. To characterize all of the candidate antiretroviral genes identified herein would take many years. Thus, we have focused on a small number of ISGs, as proof-of-principle of the usefulness of this strategy. Expression screens such as those reported herein are a powerful tool, but have weaknesses, including the potential for overexpression artifacts. However, we emphasize the fact that endogenous levels of two host factors we identify characterized herein can cause inhibition of retroviral replication. These two ISGs contribute to the anti-HIV-1 activity of IFNs via completely different mechanisms.

One antiretroviral ISG identified in our screens was IDO1. The observation that exogenous L-Trp can relieve inhibition by IDO1 and IFNγ strongly suggests that IDO1 inhibits HIV-1 through L-Trp depletion rather than through the generation of catabolites such as kynurenine. Nutrient-depletion is a recognized anti-pathogen strategy and similar effects of IDO1 have been noted for other pathogens including measles virus and hepatitis B virus (Mao et al., 2011; Obojes et al., 2005). Indeed, SAMHD1, an IFN-inducible deoxynucleoside triphosphate (dNTP) triphosphohydrolase that is also active against HIV-1, acts by depleting essential substrates required for retrovirus replication (Goldstone et al., 2011).

A simple explanation for the effects of IDO1 is that L-Trp depletion could inhibit HIV-1 by limiting the availability of L-Trp for nascent viral protein synthesis. However, it is also true that T cells can actively respond to L-Trp depletion by activating GCN2 and mTOR signaling pathways (Cobbold et al., 2009; Munn et al., 2005), which could potentially impact viral gene expression. Importantly, it is plausible that L-Trp could be sufficiently depleted in T cells in vivo to exert an antiretroviral effect. IDO1 is expressed at very high levels in APCs in HIV-1-infected patients (Favre et al., 2010), and abundant IDO1 is observed in the lymph nodes of SIV-infected macaques (Estes et al., 2006). Efficient local depletion of L-Trp by APCs could therefore inhibit HIV-1 replication in neighboring CD4+ T cells. Notably, IDO1 is sufficiently active during chronic HIV-1 infection that serum L-Trp can be 50% lower than in healthy controls (reviewed in Murray, 2003). To impact serum L-Trp levels, extreme local depletion of L-Trp likely occurs in the microenvironments (i.e., lymphoid tissues) that support viral replication. Crucially, such local depletion of L-Trp is observed in vivo. GCN2 is activated by L-Trp depletion to levels around 20-fold lower than in normal serum and this IDO-dependent GCN2 activation is readily observed in vivo (Munn et al., 2005). Thus, tissue microenvironments likely experience L-Trp depletion to an extent that could suppress HIV-1 replication.

Although L-Trp depletion has antiviral effects, elevated IDO1 activity has additional consequences in chronic HIV-1 infection (Murray, 2003; Schmidt and Schultze, 2014), as it suppresses T cell responses and promotes tolerance (Friberg et al., 2002; Munn et al., 1998; Sakurai et al., 2002). IDO1 activity has been reported to skew CD4+ T cell differentiation to regulatory T cells at the expense of Th17 cells, thereby exacerbating CD4+ Th17 depletion, perhaps leading to increased microbial translocation and systemic immune activation (Brenchley et al., 2006; Favre et al., 2010). Thus, IDO1 activity could potentially mediate inhibition of HIV-1 replication while simultaneously promoting immunosuppression.

Our screens uncovered two antiretroviral TRIM proteins, TRIM38 and TRIM56, that appear to act by regulating the establishment of an antiviral state. Other TRIM proteins can stimulate cell responses to pathogens, including TRIM25, which induces ubiquitination of RIG-I (Gack et al., 2007), and TRIM5, which has been implicated in promoting inflammatory transcription (Pertel et al., 2011). Overexpression screens have suggested that other TRIM proteins have antiretroviral activity, through unknown mechanisms (Uchil et al., 2008). While overexpressed TRIM56 did not appear to function through IFNβ or ISRE promoter elements, endogenous TRIM56 both increased the expression of many ISGs in response to IFNα and enhanced the establishment of an anti-HIV-1 state. Moreover, modest TRIM56 overexpression caused dramatic inhibition of HIV-1 replication. It is likely that these findings are causally related, although we cannot exclude the possibility that these reflect distinct activities of TRIM56, as the signaling and directly antiviral activities of tetherin and TRIM5 are clearly separable functions

(H) Adaptation of HIV-1 to GHOST-TRIM56#2 cells via spreading replication. At each discontinuity, virions harvested from the GHOST-TRIM56#2 cells were passaged onto GHOST-vector and GHOST-TRIM56#2 cells.

(I) Schematic representation and sequence analysis of an HIV-1 clone (TRIM56R) adapted to replicate in GHOST cells expressing TRIM56.

(J) WB analysis of Gag expression and particle release in GHOST vector and GHOST-TRIM56 cells, during a single cycle of HIV-1 and HIV-1/TRIM56R replication.

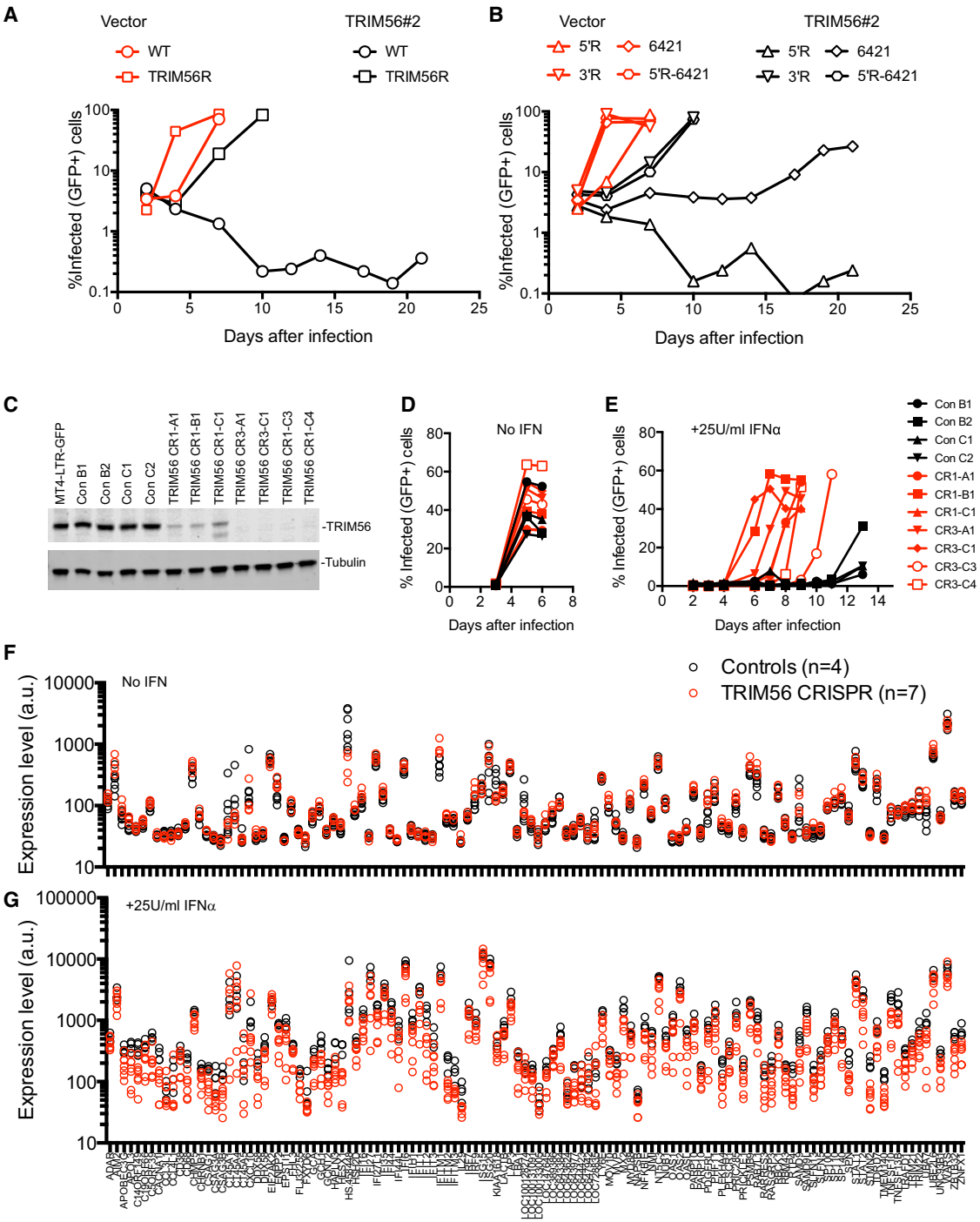

Figure 7. Multiple Viral Determinants and ISGs Underlie Inhibition of HIV-1 Replication by Endogenous TRIM56

(A and B) Spreading replication of HIV-1 and HIV-1/TRIM56R in GHOSTX4-vector and GHOSTX4-TRIM56#2 cells (A), or chimeric viruses constructed using HIV-1 and HIV-1/TRIM56R (B).

(C) WB analysis of TRIM56 expression in clones of MT4-LTR-GFP cells transduced with lentiviral vectors expressing Cas9 only or Cas9 plus one of two TRIM56-targeted guide RNAs (CR1 or CR3).

(D and E) HIV-1 replication in the absence (D) or presence (E) of 25U/ml IFNα in clones of control (n = 4) or TRIM56 knockout (n = 7) MT4-LTR-GFP cells described in (C).

(F and G) Microarray analysis of the expression levels (in a.u.) for the ~120 genes most highly induced by 25U/ml IFNα in clones of control (n = 4) or TRIM56 knockout (n = 7) MT4-LTR-GFP cells described in (C) in the presence (G) or absence (F) of IFN.

(Galão et al., 2012; Pertel et al., 2011). Previously, TRIM56 has been reported to inhibit the replication of several RNA viruses, while other RNA viruses are unaffected (Liu et al., 2014; Wang et al., 2011); it has also been reported to enhance cellular responsiveness to TLR3 signaling by binding to TRIF (Shen et al., 2012) and to enhance IFNβ production in response to dsDNA by binding to and ubiquitinating STING (Tsuchida et al., 2010). Our data are not consistent with an important role for STING-induced IFN expression as a key mediator of TRIM56 antiretroviral activity, because anti-HIV-1 activity of overexpressed TRIM56 was observed in cells that do not express STING and cGAS, and endogenous TRIM56 only exerted anti-HIV-1 activity and enhanced ISG expression following IFNα treatment. STING-independent TRIM56 antiviral activity has also been reported for influenza viruses (Liu et al., 2016). Further work will be required to determine precisely how TRIM56 functions to inhibit HIV-1 replication and whether any previously described properties are relevant to its antiretroviral activity.

The consequences of ISG expression (such as nutrient depletion) are expected to have fitness costs for the host. However, if those costs are temporary, and smaller than those imposed by viral infection, then ISG expression is ultimately beneficial to the host. Thus, these data highlight the need for caution when contemplating therapeutic interventions designed to modulate the consequences of HIV-1 infection. Multiple ISGs that are associated with immune activation, illness, and disease progression during chronic infection likely also mediate suppression of HIV-1 replication. While the antiretroviral activities of ISGs are unable to tip the balance in favor of the host during natural HIV-1 infection, it is clear the IFNs can slow or ameliorate disease in HIV-1 and other retroviral infections. The findings reported herein should inform future efforts to understand the molecular basis by which IFNs shape susceptibility to retroviral infection, disease progression, cross-species transmission, and retroviral emergence.

EXPERIMENTAL PROCEDURES

Retroviruses and Cell Lines

All the common cell lines were maintained under standard culture conditions as detailed in the Supplemental Experimental Procedures. MT4-LTR-GFP indicator cells and IFNβ1/ISRE reporter cell lines represent cell clones modified using MLV-derived retroviral vectors. ISG-expressing MT4 and GHOSTX4 cell lines were modified using lentiviral vectors. Limiting dilution was also used to generate a panel of GHOSTX4 cells, modified to express TRIM56. Replication competent proviral clones encoding GFP (PFV) or pseudotyped envelope minus derivatives of HIV-1,-1 (NHG Δ*env*), HIV-2 (HIV-2 Δ*env* EGFP), SIVmac, (SIVmac Δ*nef* Δ*env* EGFP), and SIVagmTAN (Δ*nef* Δ*env* EGFP) or multiplasmid vector systems for FIV, EIAV, HERV-K, MLV, and CERV-2 encoding GFP were used as described previously (Busnadiego et al., 2014; Kane et al., 2013). Intact proviral clones of HIV-1 (NL4-3) (M19921) and HIV-2 (ROD10), as well as GFP encoding (in place of *nef*) NHG, were used. Infectivity and replication assays were performed as described previously (Busnadiego et al., 2014; Kane et al., 2013) and as detailed in the Supplemental Experimental Procedures and Table S1.

ISG Screens

Using the same criteria used to select human ISGs (Dittmann et al., 2015; Schoggins et al., 2011), we attempted to clone ~600 macaque ISGs using RT-PCR of IFN-treated *Macaca mulatta* cell lines. The resulting macaque and extended human ISG libraries were subcloned into the pSCRPSY vector (Accession KT368137) and pcDNA-DEST40 using Gateway (Invitrogen) technology. ISG screens were conducted in a 96-well plate format using SCRPSY lentiviral transduced target cells (incoming screens, ISRE and IFNβ promoter screens) or through cotransfection of 293T cells with ISGs encoded by pcDNA-DEST40 (outgoing screens) detailed in the Supplemental Experimental Procedures and Table S1. For each ISG, the fraction of infected, ISG/TagRFP-expressing cells (incoming screens) or the yield of infectious virions (production screens) was expressed as a percentage of the mean value across all wells for the respective library in a given screen, except the MPMV incoming screen, in which values are expressed as the mean value across each plate. ISGs that affected SCRPSY lentiviral titers are shown in Figure S1A and Table S2.

CRISPR-Mediated TRIM56 Knockout

A derivative of the HIV-based retroviral vector lentiCRISPR Version 2 (Addgene, Plasmid #52961) was constructed. MT4-LTR-GFP knockout cells were derived by transduction with lentiCRISPRV2-based viruses and single-cell clones transduced with TRIM56-targeting CR1 and CR3 vectors were derived by limiting dilution.

Quantitative Western Blotting

Western blotting was performed as described previously (Busnadiego et al., 2014; Kane et al., 2013) and detailed in the Supplemental Experimental Procedures using cell lysates and material pelleted through 20% sucrose. Antigens were visualized using secondary antibodies labeled with IRDye 800CW or IRDye 680RD (LI-COR Biosciences or Thermo Scientific) and the relevant primary antibody and scanned using a Li-Cor Odyssey Scanner.

Microarray Analysis

Total RNA was extracted, using the RNeasy Plus Mini Kit (QIAGEN), from MT4-LTR-GFP cells, control subclones, and CRISPR knockout subclones that were untreated or treated with 25 U/ml IFNα (Sigma) for 24 hr before harvest. cRNA was prepared and probed using Human HT12 Expression Beadchip (Illumina), containing ~48,000 transcript probes, according to the manufacturer's instructions.

SUPPLEMENTAL INFORMATION

Supplemental Information includes seven figures, five tables, and Supplemental Experimental Procedures and can be found with this article at http://dx.doi.org/10.1016/j.chom.2016.08.005.

AUTHOR CONTRIBUTIONS

Conceptualization, P.D.B.; Library Construction, S.J.W., M.A., and J.S.; Screening, S.J.W., M.K., F.Z., M.A., and T.K.; IDO1, S.J.R.; TRIM56, T.M.Z.; Resources, J.S. and C.M.R.; Writing – Original Draft, S.J.W. and P.D.B.; Writing – Review & Editing, M.K., T.M.Z., S.J.R., F.Z., T.K., J.S., C.M.R., S.J.W., and P.D.B.; Funding Acquisition, P.D.B., S.J.W., M.K., J.S., and C.M.R.; Supervision, P.D.B. and S.J.W.

ACKNOWLEDGMENTS

We thank Steven Soll for CERV2/MLV chimeric Gag-Pol, Nick J. Loman and Shalini Yadav for assistance, and the Developmental Studies Hybridoma Bank, University of Iowa, and NIH AIDS reagents program for antibodies. This work was supported by grants from the NIH R3764003 (to P.D.B.), 1F32AI116263-01 (to M.K.), AI091707 (to J.S. and C.M.R.), and UK MRC MR/K024752/1 (to S.J.W.). The content of this piece is solely the responsibility of the authors and does not necessarily represent the official views of the National Institutes of Health.

Received: April 25, 2016
Revised: July 5, 2016
Accepted: July 27, 2016
Published: September 14, 2016

REFERENCES

Asmuth, D.M., Murphy, R.L., Rosenkranz, S.L., Lertora, J.J., Kottilil, S., Cramer, Y., Chan, E.S., Schooley, R.T., Rinaldo, C.R., Thielman, N.,

et al.; AIDS Clinical Trials Group A5192 Team (2010). Safety, tolerability, and mechanisms of antiretroviral activity of pegylated interferon Alfa-2a in HIV-1-monoinfected participants: a phase II clinical trial. J. Infect. Dis. *201*, 1686–1696.

Bitzegeio, J., Sampias, M., Bieniasz, P.D., and Hatziioannou, T. (2013). Adaptation to the interferon-induced antiviral state by human and simian immunodeficiency viruses. J. Virol. *87*, 3549–3560.

Brenchley, J.M., Price, D.A., Schacker, T.W., Asher, T.E., Silvestri, G., Rao, S., Kazzaz, Z., Bornstein, E., Lambotte, O., Altmann, D., et al. (2006). Microbial translocation is a cause of systemic immune activation in chronic HIV infection. Nat. Med. *12*, 1365–1371.

Busnadiego, I., Kane, M., Rihn, S.J., Preugschas, H.F., Hughes, J., Blanco-Melo, D., Strouvelle, V.P., Zang, T.M., Willett, B.J., Boutell, C., et al. (2014). Host and viral determinants of Mx2 antiretroviral activity. J. Virol. *88*, 7738–7752.

Cobbold, S.P., Adams, E., Farquhar, C.A., Nolan, K.F., Howie, D., Lui, K.O., Fairchild, P.J., Mellor, A.L., Ron, D., and Waldmann, H. (2009). Infectious tolerance via the consumption of essential amino acids and mTOR signaling. Proc. Natl. Acad. Sci. USA *106*, 12055–12060.

Dittmann, M., Hoffmann, H.H., Scull, M.A., Gilmore, R.H., Bell, K.L., Ciancanelli, M., Wilson, S.J., Crotta, S., Yu, Y., Flatley, B., et al. (2015). A serpin shapes the extracellular environment to prevent influenza A virus maturation. Cell *160*, 631–643.

Doyle, T., Goujon, C., and Malim, M.H. (2015). HIV-1 and interferons: who's interfering with whom? Nat. Rev. Microbiol. *13*, 403–413.

Estes, J.D., Li, Q., Reynolds, M.R., Wietgrefe, S., Duan, L., Schacker, T., Picker, L.J., Watkins, D.I., Lifson, J.D., Reilly, C., et al. (2006). Premature induction of an immunosuppressive regulatory T cell response during acute simian immunodeficiency virus infection. J. Infect. Dis. *193*, 703–712.

Favre, D., Mold, J., Hunt, P.W., Kanwar, B., Loke, P., Seu, L., Barbour, J.D., Lowe, M.M., Jayawardene, A., Aweeka, F., et al. (2010). Tryptophan catabolism by indoleamine 2,3-dioxygenase 1 alters the balance of TH17 to regulatory T cells in HIV disease. Sci. Transl. Med. *2*, 32ra36.

Fenton-May, A.E., Dibben, O., Emmerich, T., Ding, H., Pfafferott, K., Aasa-Chapman, M.M., Pellegrino, P., Williams, I., Cohen, M.S., Gao, F., et al. (2013). Relative resistance of HIV-1 founder viruses to control by interferon-alpha. Retrovirology *10*, 146.

Friberg, M., Jennings, R., Alsarraj, M., Dessureault, S., Cantor, A., Extermann, M., Mellor, A.L., Munn, D.H., and Antonia, S.J. (2002). Indoleamine 2,3-dioxygenase contributes to tumor cell evasion of T cell-mediated rejection. International journal of cancer Journal international du cancer *101*, 151–155.

Gack, M.U., Shin, Y.C., Joo, C.H., Urano, T., Liang, C., Sun, L., Takeuchi, O., Akira, S., Chen, Z., Inoue, S., and Jung, J.U. (2007). TRIM25 RING-finger E3 ubiquitin ligase is essential for RIG-I-mediated antiviral activity. Nature *446*, 916–920.

Galão, R.P., Le Tortorec, A., Pickering, S., Kueck, T., and Neil, S.J. (2012). Innate sensing of HIV-1 assembly by Tetherin induces NFκB-dependent proinflammatory responses. Cell Host Microbe *12*, 633–644.

Goldstone, D.C., Ennis-Adeniran, V., Hedden, J.J., Groom, H.C., Rice, G.I., Christodoulou, E., Walker, P.A., Kelly, G., Haire, L.F., Yap, M.W., et al. (2011). HIV-1 restriction factor SAMHD1 is a deoxynucleoside triphosphate triphosphohydrolase. Nature *480*, 379–382.

Hammer, S.M., Gillis, J.M., Groopman, J.E., and Rose, R.M. (1986). In vitro modification of human immunodeficiency virus infection by granulocyte-macrophage colony-stimulating factor and gamma interferon. Proc. Natl. Acad. Sci. USA *83*, 8734–8738.

Hassanain, H.H., Chon, S.Y., and Gupta, S.L. (1993). Differential regulation of human indoleamine 2,3-dioxygenase gene expression by interferons-gamma and -alpha. Analysis of the regulatory region of the gene and identification of an interferon-gamma-inducible DNA-binding factor. J. Biol. Chem. *268*, 5077–5084.

Hatziioannou, T., and Bieniasz, P.D. (2011). Antiretroviral restriction factors. Curr. Opin. Virol. *1*, 526–532.

Hayaishi, O. (1976). Properties and function of indoleamine 2,3-dioxygenase. J. Biochem. *79*, 13P–21P.

Kane, M., Yadav, S.S., Bitzegeio, J., Kutluay, S.B., Zang, T., Wilson, S.J., Schoggins, J.W., Rice, C.M., Yamashita, M., Hatziioannou, T., and Bieniasz, P.D. (2013). MX2 is an interferon-induced inhibitor of HIV-1 infection. Nature *502*, 563–566.

Liu, B., Li, N.L., Wang, J., Shi, P.Y., Wang, T., Miller, M.A., and Li, K. (2014). Overlapping and distinct molecular determinants dictating the antiviral activities of TRIM56 against flaviviruses and coronavirus. J. Virol. *88*, 13821–13835.

Liu, B., Li, N.L., Shen, Y., Bao, X., Fabrizio, T., Elbahesh, H., Webby, R.J., and Li, K. (2016). The C-Terminal Tail of TRIM56 Dictates Antiviral Restriction of Influenza A and B Viruses by Impeding Viral RNA Synthesis. J. Virol. *90*, 4369–4382.

Mao, R., Zhang, J., Jiang, D., Cai, D., Levy, J.M., Cuconati, A., Block, T.M., Guo, J.T., and Guo, H. (2011). Indoleamine 2,3-dioxygenase mediates the antiviral effect of gamma interferon against hepatitis B virus in human hepatocyte-derived cells. J. Virol. *85*, 1048–1057.

Munn, D.H., Zhou, M., Attwood, J.T., Bondarev, I., Conway, S.J., Marshall, B., Brown, C., and Mellor, A.L. (1998). Prevention of allogeneic fetal rejection by tryptophan catabolism. Science *281*, 1191–1193.

Munn, D.H., Sharma, M.D., Baban, B., Harding, H.P., Zhang, Y., Ron, D., and Mellor, A.L. (2005). GCN2 kinase in T cells mediates proliferative arrest and anergy induction in response to indoleamine 2,3-dioxygenase. Immunity *22*, 633–642.

Murray, M.F. (2003). Tryptophan depletion and HIV infection: a metabolic link to pathogenesis. Lancet Infect. Dis. *3*, 644–652.

Obojes, K., Andres, O., Kim, K.S., Däubener, W., and Schneider-Schaulies, J. (2005). Indoleamine 2,3-dioxygenase mediates cell type-specific anti-measles virus activity of gamma interferon. J. Virol. *79*, 7768–7776.

Opitz, C.A., Litzenburger, U.M., Sahm, F., Ott, M., Tritschler, I., Trump, S., Schumacher, T., Jestaedt, L., Schrenk, D., Weller, M., et al. (2011). An endogenous tumour-promoting ligand of the human aryl hydrocarbon receptor. Nature *478*, 197–203.

Pauls, E., Ruiz, A., Riveira-Muñoz, E., Permanyer, M., Badia, R., Clotet, B., Keppler, O.T., Ballana, E., and Este, J.A. (2014). p21 regulates the HIV-1 restriction factor SAMHD1. Proc. Natl. Acad. Sci. USA *111*, E1322–E1324.

Pertel, T., Hausmann, S., Morger, D., Züger, S., Guerra, J., Lascano, J., Reinhard, C., Santoni, F.A., Uchil, P.D., Chatel, L., et al. (2011). TRIM5 is an innate immune sensor for the retrovirus capsid lattice. Nature *472*, 361–365.

Pfefferkorn, E.R. (1984). Interferon gamma blocks the growth of Toxoplasma gondii in human fibroblasts by inducing the host cells to degrade tryptophan. Proc. Natl. Acad. Sci. USA *81*, 908–912.

Sakurai, K., Zou, J.P., Tschetter, J.R., Ward, J.M., and Shearer, G.M. (2002). Effect of indoleamine 2,3-dioxygenase on induction of experimental autoimmune encephalomyelitis. J. Neuroimmunol. *129*, 186–196.

Sandler, N.G., Bosinger, S.E., Estes, J.D., Zhu, R.T., Tharp, G.K., Boritz, E., Levin, D., Wijeyesinghe, S., Makamdop, K.N., del Prete, G.Q., et al. (2014). Type I interferon responses in rhesus macaques prevent SIV infection and slow disease progression. Nature *511*, 601–605.

Schmidt, S.V., and Schultze, J.L. (2014). New Insights into IDO Biology in Bacterial and Viral Infections. Front. Immunol. *5*, 384.

Schoggins, J.W., Wilson, S.J., Panis, M., Murphy, M.Y., Jones, C.T., Bieniasz, P., and Rice, C.M. (2011). A diverse range of gene products are effectors of the type I interferon antiviral response. Nature *472*, 481–485.

Schoggins, J.W., MacDuff, D.A., Imanaka, N., Gainey, M.D., Shrestha, B., Eitson, J.L., Mar, K.B., Richardson, R.B., Ratushny, A.V., Litvak, V., et al. (2014). Pan-viral specificity of IFN-induced genes reveals new roles for cGAS in innate immunity. Nature *505*, 691–695.

Shen, Y., Li, N.L., Wang, J., Liu, B., Lester, S., and Li, K. (2012). TRIM56 is an essential component of the TLR3 antiviral signaling pathway. J. Biol. Chem. *287*, 36404–36413.

Stetson, D.B., and Medzhitov, R. (2006). Type I interferons in host defense. Immunity *25*, 373–381.

Tsuchida, T., Zou, J., Saitoh, T., Kumar, H., Abe, T., Matsuura, Y., Kawai, T., and Akira, S. (2010). The ubiquitin ligase TRIM56 regulates innate immune responses to intracellular double-stranded DNA. Immunity *33*, 765–776.

Uchil, P.D., Quinlan, B.D., Chan, W.T., Luna, J.M., and Mothes, W. (2008). TRIM E3 ligases interfere with early and late stages of the retroviral life cycle. PLoS Pathog. *4*, e16.

Wang, J., Liu, B., Wang, N., Lee, Y.M., Liu, C., and Li, K. (2011). TRIM56 is a virus- and interferon-inducible E3 ubiquitin ligase that restricts pestivirus infection. J. Virol. *85*, 3733–3745.

Wilson, S.J., Schoggins, J.W., Zang, T., Kutluay, S.B., Jouvenet, N., Alim, M.A., Bitzegeio, J., Rice, C.M., and Bieniasz, P.D. (2012). Inhibition of HIV-1 particle assembly by 2′,3′-cyclic-nucleotide 3′-phosphodiesterase. Cell Host Microbe *12*, 585–597.

Cell Host & Microbe, Volume *20*

Supplemental Information

Identification of Interferon-Stimulated Genes with Antiretroviral Activity

Melissa Kane, Trinity M. Zang, Suzannah J. Rihn, Fengwen Zhang, Tonya Kueck, Mudathir Alim, John Schoggins, Charles M. Rice, Sam J. Wilson, and Paul D. Bieniasz

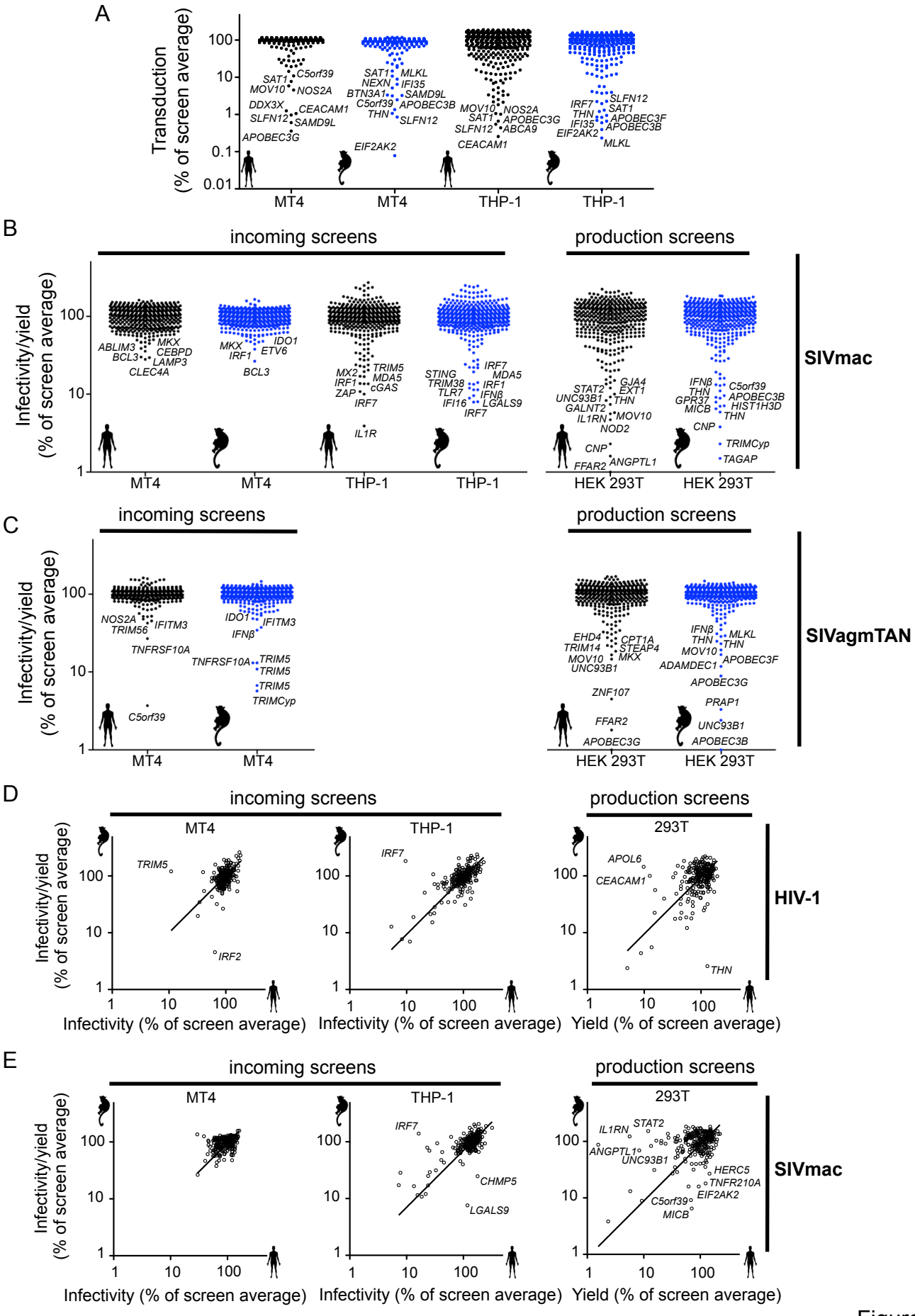
A
Transduction (% of screen average)
100
10
1
0.1
0.01
SAT1
C5orf39
MOV10
NOS2A
DDX3X
CEACAM1
SLFN12
SAMD9L
APOBEC3G
SAT1
MLKL
NEXN
IFI35
BTN3A1
SAMD9L
C5orf39
APOBEC3B
THN
SLFN12
EIF2AK2
MOV10
NOS2A
SAT1
APOBEC3G
SLFN12
ABCA9
CEACAM1
IRF7
SLFN12
THN
SAT1
IFI35
APOBEC3F
EIF2AK2
APOBEC3B
MLKL
MT4
MT4
THP-1
THP-1
B
incoming screens
production screens
Infectivity/yield (% of screen average)
100
10
1
ABLIM3
MKX
BCL3
CEBPD
LAMP3
CLEC4A
MKX
IDO1
IRF1
ETV6
BCL3
MX2
TRIM5
IRF1
MDA5
ZAP
cGAS
IRF7
IL1R
STING
IRF7
TRIM38
MDA5
TLR7
IRF1
IFI16
IFNβ
LGALS9
IRF7
STAT2
GJA4
UNC93B1
EXT1
GALNT2
THN
IL1RN
MOV10
NOD2
CNP
FFAR2
ANGPTL1
IFNβ
C5orf39
THN
APOBEC3B
GPR37
HIST1H3D
MICB
THN
CNP
TRIMCyp
TAGAP
MT4
MT4
THP-1
THP-1
HEK 293T
HEK 293T
SIVmac
C
incoming screens
production screens
Infectivity/yield (% of screen average)
100
10
1
NOS2A
IFITM3
TRIM56
TNFRSF10A
IDO1
IFITM3
IFNβ
TNFRSF10A
TRIM5
TRIM5
TRIM5
TRIMCyp
C5orf39
EHD4
CPT1A
TRIM14
STEAP4
MOV10
MKX
UNC93B1
ZNF107
FFAR2
APOBEC3G
IFNβ
MLKL
THN
THN
MOV10
APOBEC3F
ADAMDEC1
APOBEC3G
PRAP1
UNC93B1
APOBEC3B
MT4
MT4
HEK 293T
HEK 293T
SIVagmTAN
D
incoming screens
production screens
MT4
THP-1
293T
Infectivity/yield (% of screen average)
100
10
1
TRIM5
IRF2
IRF7
APOL6
CEACAM1
THN
1
10
100
Infectivity (% of screen average)
Infectivity (% of screen average)
Yield (% of screen average)
HIV-1
E
incoming screens
production screens
MT4
THP-1
293T
Infectivity/yield (% of screen average)
100
10
1
IRF7
CHMP5
LGALS9
IL1RN
STAT2
ANGPTL1
UNC93B1
HERC5
TNFR210A
EIF2AK2
C5orf39
MICB
1
10
100
Infectivity (% of screen average)
Infectivity (% of screen average)
Yield (% of screen average)
SIVmac

Figure S1

Fig S1. Effects of human and macaque ISGs on vector production and primate lentiviruses (Related to Figure 1).

(A) Effects of ISG encoding vectors on vector transduction in MT4 and THP-1 cells.

(B, C) Effects of ISGs in incoming screens with SIVmac (B) in MT4 and THP-1 cells; and SIVagmTAN, (C) in MT4 cells only, and effects of the same ISGs on the generation of infectious SIVmac (B) and SIVagmTAN (C) particles in 293T cells.

(D, E) Comparison of the effects of human and macaque ISGs (genes in both libraries) in incoming screens with HIV-1 (D) and SIVmac (E) in MT4 and THP-1 cells, and effects of the same ISGs on the generation of infectious HIV-1 (D) and SIVmac (E) from 293T cells. All screens were normalised to the screen average (100 arbitrary units).

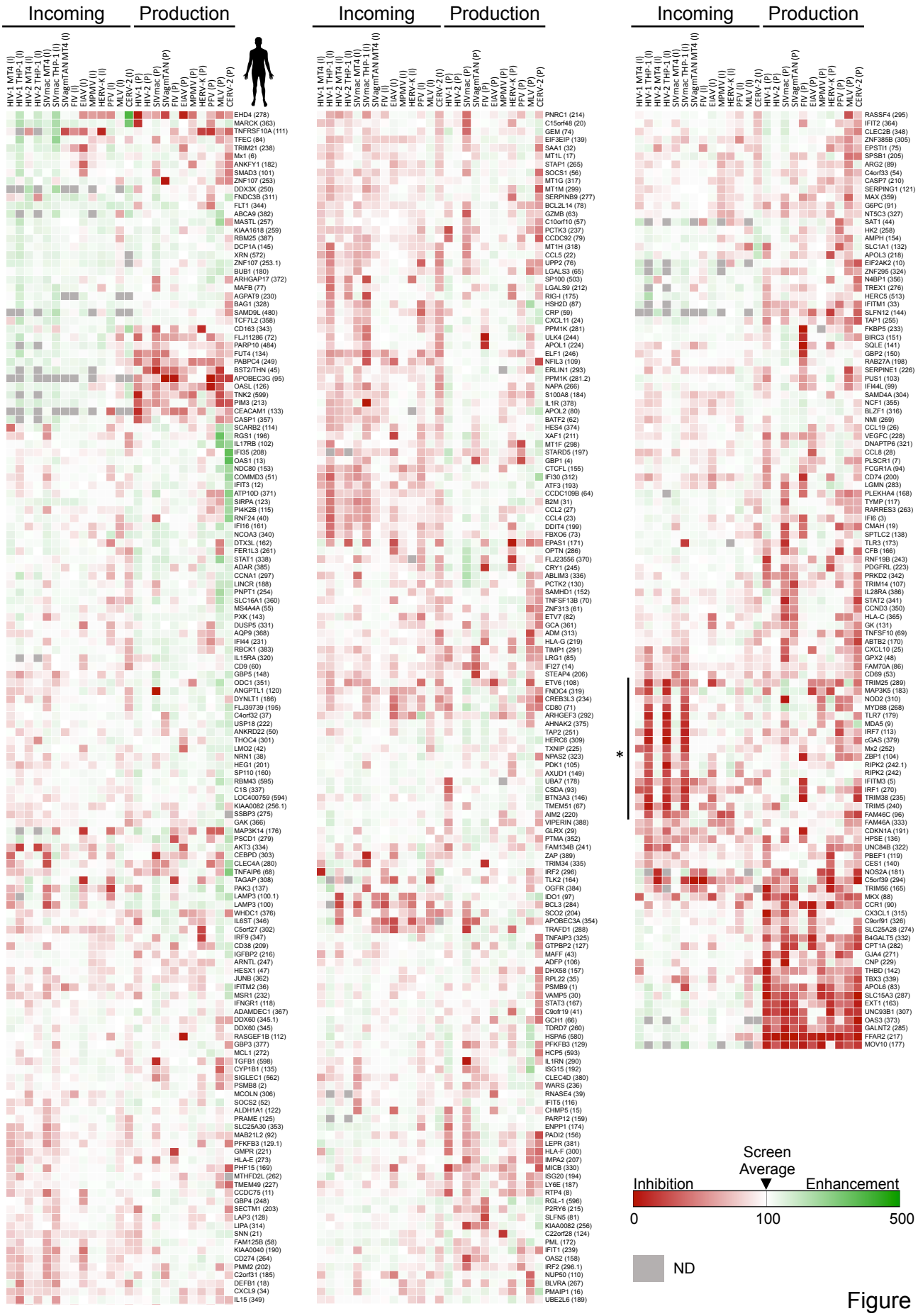
Incoming
Production
HIV-1 MT4 (I)
HIV-1 THP-1 (I)
HIV-2 MT4 (I)
HIV-2 THP-1 (I)
SIVmac MT4 (I)
SIVmac THP-1 (I)
SIVagmTAN MT4 (I)
FIV (I)
EIAV (I)
MPMV (I)
HERV-K (I)
PFV (I)
MLV (I)
CERV-2 (I)
HIV-1 (P)
HIV-2 (P)
SIVmac (P)
SIVagmTAN (P)
FIV (P)
EIAV (P)
MPMV (P)
HERV-K (P)
PFV (P)
MLV (P)
CERV-2 (P)
EHD4 (278)
MARCK (363)
TNFRSF10A (111)
TFEC (84)
TRIM21 (238)
Mx1 (6)
ANKFY1 (182)
SMAD3 (101)
ZNF107 (253)
DDX3X (250)
FNDC3B (311)
FLT1 (344)
ABCA9 (382)
MASTL (257)
KIAA1618 (259)
RBM25 (387)
DCP1A (145)
XRN (572)
ZNF107 (253.1)
BUB1 (180)
ARHGAP17 (372)
MAFB (77)
AGPAT9 (230)
BAG1 (328)
SAMD9L (480)
TCF7L2 (358)
CD163 (343)
FLJ11286 (72)
PARP10 (484)
FUT4 (134)
PABPC4 (249)
BST2/THN (45)
APOBEC3G (95)
OASL (126)
TNK2 (599)
PIM3 (213)
CEACAM1 (133)
CASP1 (357)
SCARB2 (114)
RGS1 (196)
IL17RB (102)
IFI35 (208)
OAS1 (13)
NDC80 (153)
COMMD3 (51)
IFIT3 (12)
ATP10D (371)
SIRPA (123)
PI4K2B (115)
RNF24 (40)
IFI16 (161)
NCOA3 (340)
DTX3L (162)
FER1L3 (261)
STAT1 (338)
ADAR (385)
CCNA1 (297)
LINCR (188)
PNPT1 (254)
SLC16A1 (360)
MS4A4A (55)
PXK (143)
DUSP5 (331)
AQP9 (368)
IFI44 (231)
RBCK1 (383)
IL15RA (320)
CD9 (60)
GBP5 (148)
ODC1 (351)
ANGPTL1 (120)
DYNLT1 (186)
FLJ39739 (195)
C4orf32 (37)
USP18 (222)
ANKRD22 (50)
THOC4 (301)
LMO2 (42)
NRN1 (38)
HEG1 (201)
SP110 (160)
RBM43 (595)
C1S (337)
LOC400759 (594)
KIAA0082 (256.1)
SSBP3 (275)
GAK (366)
MAP3K14 (176)
PSCD1 (279)
AKT3 (334)
CEBPD (303)
CLEC4A (280)
TNFAIP6 (68)
TAGAP (308)
PAK3 (137)
LAMP3 (100.1)
LAMP3 (100)
WHDC1 (376)
IL6ST (346)
C5orf27 (302)
IRF9 (347)
CD38 (209)
IGFBP2 (216)
ARNTL (247)
HESX1 (47)
JUNB (362)
IFITM2 (36)
MSR1 (232)
IFNGR1 (118)
ADAMDEC1 (367)
DDX60 (345.1)
DDX60 (345)
RASGEF1B (112)
GBP3 (377)
MCL1 (272)
TGFB1 (598)
CYP1B1 (135)
SIGLEC1 (562)
PSMB8 (2)
MCOLN (306)
SOCS2 (52)
ALDH1A1 (122)
PRAME (125)
SLC25A30 (353)
MAB21L2 (92)
PFKFB3 (129.1)
GMPR (221)
HLA-E (273)
PHF15 (169)
MTHFD2L (262)
TMEM49 (227)
CCDC75 (11)
GBP4 (248)
SECTM1 (203)
LAP3 (128)
LIPA (314)
SNN (21)
FAM125B (58)
KIAA0040 (190)
CD274 (264)
PMM2 (202)
C2orf31 (185)
DEFB1 (18)
CXCL9 (34)
IL15 (349)
PNRC1 (214)
C15orf48 (20)
GEM (74)
EIF3EIP (139)
SAA1 (32)
MT1L (17)
STAP1 (265)
SOCS1 (56)
MT1G (317)
MT1M (299)
SERPINB9 (277)
BCL2L14 (78)
GZMB (63)
C10orf10 (57)
PCTK3 (237)
CCDC92 (79)
MTTH (318)
CCL5 (22)
UPP2 (76)
LGALS3 (65)
SP100 (503)
LGALS9 (212)
RNASE6 (175)
HSH2D (87)
CRP (59)
CXCL11 (24)
PPM1K (281)
ULK4 (244)
APOL1 (224)
ELF1 (246)
NFIL3 (109)
ERLIN1 (293)
PPM1K (281.2)
NAPA (266)
S100A8 (184)
IL1R (378)
APOL2 (80)
BATF2 (62)
HES4 (374)
XAF1 (211)
MT1F (298)
STARD5 (197)
GBP1 (4)
CTCFL (155)
IFI30 (312)
ATF3 (193)
CCDC109B (64)
B2M (31)
CCL2 (27)
CCL4 (23)
DDIT4 (199)
FBXO6 (73)
EPAS1 (171)
OPTN (286)
FLJ23556 (370)
CRY1 (245)
ABLIM3 (336)
PCTK2 (130)
SAMHD1 (152)
TNFSF13B (70)
ZNF313 (61)
ETV7 (82)
GCA (361)
ADM (313)
HLA-G (219)
TIMP1 (291)
LRG1 (85)
IFI27 (14)
STEAP4 (206)
ETV6 (108)
FNDC4 (319)
CREB3L3 (234)
CD80 (71)
ARHGEF3 (292)
AHNAK2 (375)
TAP2 (251)
HERC6 (309)
TXNIP (225)
NPAS2 (323)
PDK1 (105)
AXUD1 (149)
UBA7 (178)
CSDA (93)
BTN3A3 (146)
TMEM51 (67)
AIM2 (220)
VIPERIN (388)
GLRX (29)
PTMA (352)
FAM134B (241)
ZAP (389)
TRIM34 (335)
IRF7 (296)
TLK2 (164)
OGFR (384)
IDO1 (97)
BCL3 (284)
SCO2 (204)
APOBEC3A (354)
TRAFD1 (288)
TNFAIP3 (325)
GTPBP2 (127)
MAFF (43)
ADFP (106)
HERC5 (157)
RPL22 (35)
PSMB9 (1)
VAMP5 (30)
STAT3 (167)
C9orf19 (41)
GCH1 (66)
TDRD7 (260)
HSPA6 (580)
PFKFB3 (129)
HCP5 (593)
IL1RN (290)
ISG15 (192)
CLEC4D (380)
WARS (236)
RNASE4 (39)
IFIT5 (116)
CH25H (15)
PARP12 (159)
ENPP1 (174)
PADI2 (156)
LEPR (381)
HLA-F (300)
IMPA2 (207)
MICB (330)
ISG20 (194)
LY6E (187)
RTP4 (8)
RGL-1 (596)
PSRC1 (215)
SLFN5 (81)
KIAA0082 (256)
C22orf28 (124)
PML (172)
IFIT1 (239)
OAS2 (158)
IRF2 (296.1)
NUP50 (110)
BLVRA (267)
PMAIP1 (16)
UBE2L6 (189)
RASSF4 (295)
IFIT2 (364)
CLEC2B (348)
ZNF385B (305)
EPSTI1 (75)
SPSB1 (205)
ARG2 (89)
C4orf33 (54)
CASP7 (210)
SERPING1 (121)
MAX (359)
G6PC (91)
NT5C3 (327)
SAT1 (44)
HK2 (258)
AMPH (154)
SLC1A1 (132)
APOL3 (218)
EIF2AK2 (10)
ZNF295 (324)
N4BP1 (356)
TREX1 (276)
HERC5 (513)
IFITM1 (33)
SLFN12 (144)
TAP1 (255)
FKBP5 (233)
BIRC3 (151)
SQLE (141)
GBP2 (150)
RAB27A (198)
SERPINE1 (226)
PUS1 (103)
IFI44L (99)
SAMD4A (304)
NCF1 (355)
BLZF1 (316)
NMI (269)
CCL19 (26)
VEGFC (228)
DNAPTP6 (321)
CCL8 (28)
PLSCR1 (7)
FCGR1A (94)
CD74 (200)
LGMN (283)
PLEKHA4 (168)
TYMP (117)
RARRES3 (263)
IFI6 (3)
CMAH (19)
SPTLC2 (138)
TLR3 (173)
CFB (166)
RNF19B (243)
PDGFRL (223)
PRKD2 (342)
TRIM14 (107)
IL28RA (386)
STAT2 (341)
CCND3 (350)
HLA-C (365)
GK (131)
TNFSF10 (69)
ABTB2 (170)
CXCL10 (25)
GPX2 (48)
FAM70A (86)
CD69 (53)
TRIM25 (289)
MAP3K5 (183)
NOD2 (310)
MYD88 (268)
TLR7 (179)
MDA5 (9)
IRF7 (113)
cGAS (379)
Mx2 (252)
ZBP1 (104)
RIPK2 (242.1)
RIPK2 (242)
IFITM3 (5)
IRF1 (270)
TRIM38 (235)
TRIM5 (240)
FAM46C (96)
FAM46A (333)
CDKN1A (191)
HPSE (136)
UNC84B (322)
PBEF1 (119)
CES1 (140)
NOS2A (181)
C5orf39 (294)
TRIM56 (165)
MKX (88)
CCR1 (90)
CX3CL1 (315)
C9orf91 (326)
SLC25A28 (274)
B4GALT5 (332)
CPT1A (282)
GJA4 (271)
CNP (229)
THBD (142)
TBX3 (339)
APOL6 (83)
SLC15A3 (287)
EXT1 (163)
UNC93B1 (307)
OAS3 (373)
GALNT2 (285)
FFAR2 (217)
MOV10 (177)
*
Screen Average
Inhibition
Enhancement
0
100
500
ND

Figure S2

Figure S2. Heat map representing effects of human ISGs on retroviral infection (Related to Figure 1 and Figure 2). The effect of ISGs in the 25 incoming and outgoing screens represented in a heat map. All screens were normalised to the screen average (100 arbitrary units) with inhibition indicated in red and enhancement in green. Absent data, due to inefficient transduction, is indicated in grey (ND). Where allelic variants, spliced variants and repeated genes occur in the library, all data is presented and represent separate values from distinct transduction/transfection events. Asterisks denote clusters of ISGs whose protective effect is most evident in THP-1 cells. Heatmaps were produced using Gitools 2.2 and genes were hierarchically clustered using Manhattan maximum distance.

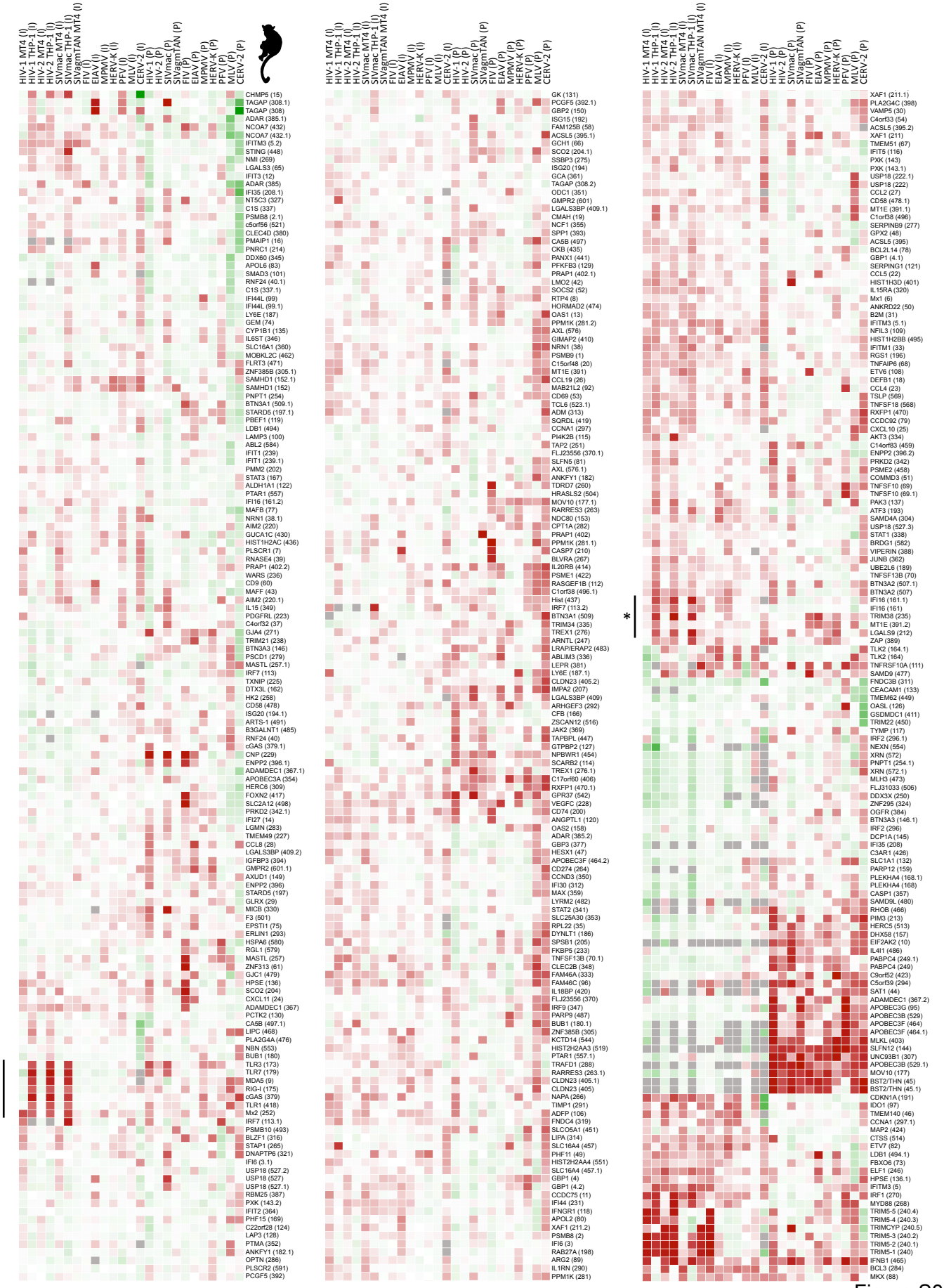
Incoming
Production
HIV-1 MT4 (I)
HIV-1 THP-1 (I)
HIV-2 MT4 (I)
HIV-2 THP-1 (I)
SIVmac MT4 (I)
SIVmac THP-1 (I)
SIVagmTAN MT4 (I)
FIV (I)
EIAV (I)
MPMV (I)
HERV-K (I)
PFV (I)
MLV (I)
CERV-2 (I)
HIV-1 (P)
HIV-2 (P)
SIVmac (P)
SIVagmTAN (P)
FIV (P)
EIAV (P)
MPMV (P)
HERV-K (P)
PFV (P)
MLV (P)
CERV-2 (P)
CHMP5 (15)
TAGAP (308.1)
TAGAP (308)
ADAR (385.1)
NCOA7 (432)
NCOA7 (432.1)
IFITM3 (5.2)
STING (448)
NMI (269)
LGALS3 (65)
IFIT3 (12)
ADAR (385)
IFI35 (208.1)
NT5C3 (327)
C1S (337)
PSMB8 (2.1)
c5orf56 (521)
CLEC4D (380)
PMAIP1 (16)
PNRC1 (214)
DDX60 (345)
APOL6 (83)
SMAD3 (101)
RNF24 (40.1)
C1S (337.1)
IFI44L (99)
IFI44L (99.1)
LY6E (187)
GEM (74)
CYP1B1 (135)
IL6ST (346)
SLC16A1 (360)
MOBKL2C (462)
FLRT3 (471)
ZNF385B (305.1)
SAMHD1 (152.1)
SAMHD1 (152)
PNPT1 (254)
BTN3A1 (509.1)
STARD5 (197.1)
PBEF1 (119)
LDB1 (494)
LAMP3 (100)
ABL2 (584)
IFIT1 (239)
IFIT1 (239.1)
PMM2 (202)
STAT3 (167)
ALDH1A1 (122)
PTAR1 (557)
IFI16 (161.2)
MAFB (77)
NRN1 (38.1)
AIM2 (220)
GUCA1C (430)
HIST1H2AC (436)
PLSCR1 (7)
RNASE4 (39)
PRAP1 (402.2)
WARS (236)
CD9 (60)
MAFF (43)
AIM2 (220.1)
IL15 (349)
PDGFRL (223)
C4orf32 (37)
GJA4 (271)
TRIM21 (238)
BTN3A3 (146)
PSCD1 (279)
MASTL (257.1)
IRF7 (113)
TXNIP (225)
DTX3L (162)
HK2 (258)
CD58 (478)
ISG20 (194.1)
ARTS-1 (491)
B3GALNT1 (485)
RNF24 (40)
cGAS (379.1)
CNP (229)
ENPP2 (396.1)
ADAMDEC1 (367.1)
APOBEC3A (354)
HERC6 (309)
FOXN2 (417)
SLC2A12 (498)
PRKD2 (342.1)
IFI27 (14)
LGMN (283)
TMEM49 (227)
CCL8 (28)
LGALS3BP (409.2)
IGFBP3 (394)
GMPR2 (601.1)
AXUD1 (149)
ENPP2 (396)
STARD5 (197)
GLRX (29)
MICB (330)
F3 (501)
EPSTI1 (75)
ERLIN1 (293)
HSPA6 (580)
RGL1 (579)
MASTL (257)
ZNF313 (61)
GJC1 (479)
HPSE (136)
SCO2 (204)
CXCL11 (24)
ADAMDEC1 (367)
PCTK2 (130)
CA5B (497.1)
LIPC (468)
PLA2G4A (476)
NBN (553)
BUB1 (180)
TLR3 (173)
TLR7 (179)
MDA5 (9)
RIG-I (175)
cGAS (379)
TLR1 (418)
Mx2 (252)
IRF7 (113.1)
PSMB10 (493)
BLZF1 (316)
STAP1 (265)
DNAPTP6 (321)
IFI6 (3.1)
USP18 (527.2)
USP18 (527)
USP18 (527.1)
RBM25 (387)
PXK (143.2)
IFIT2 (364)
PHF15 (169)
C22orf28 (124)
LAP3 (128)
PTMA (352)
ANKFY1 (182.1)
OPTN (286)
PLSCR2 (591)
PCGF5 (392)
GK (131)
PCGF5 (392.1)
GBP2 (150)
ISG15 (192)
FAM125B (58)
ACSL5 (395.1)
GCH1 (66)
SCO2 (204.1)
SSBP3 (275)
ISG20 (194)
GCA (361)
TAGAP (308.2)
ODC1 (351)
GMPR2 (601)
LGALS3BP (409.1)
CMAH (19)
NCF1 (355)
SPP1 (393)
CA5B (497)
OKB (435)
PANX1 (441)
PFKFB3 (129)
PRAP1 (402.1)
LMO2 (42)
SOCS2 (52)
RTP4 (8)
HORMAD2 (474)
OAS1 (13)
PPM1K (281.2)
AXL (576)
GIMAP2 (410)
NRN1 (38)
PSMB9 (1)
C15orf48 (20)
MT1E (391)
CCL19 (26)
MAB21L2 (92)
CD69 (53)
TCL6 (523.1)
ADM (313)
SQRDL (419)
CCNA1 (297)
PI4KB (115)
TAP2 (251)
FLJ23556 (370.1)
SLFN5 (81)
AXL (576.1)
ANKFY1 (182)
TDRD7 (260)
HRASLS2 (504)
MOV10 (177.1)
RARRES3 (263)
NDC80 (153)
CPT1A (282)
PRAP1 (402)
PPM1K (281.1)
CASP7 (210)
BLVRA (267)
IL20RB (414)
PSME1 (422)
RASGEF1B (112)
C1orf38 (496.1)
Hist (437)
IRF7 (113.2)
BTN3A1 (509)
TRIM34 (335)
TREX1 (276)
ARNTL (247)
LRAP/ERAP2 (483)
ABLIM3 (336)
LEPR (381)
LY86 (187.1)
CLDN23 (405.2)
IMPA2 (207)
LGALS3BP (409)
ARHGEF3 (292)
CFB (166)
ZSCAN18 (516)
JAK2 (369)
TAPBPL (447)
GTPBP2 (127)
NPBWR1 (454)
SCARB2 (114)
TRF2E (276.1)
C17orf60 (406)
RXFP1 (470.1)
GPR37 (542)
VEGFC (228)
CD74 (200)
ANXA2 (120)
OAS2 (158)
ADAR (385.2)
GBP3 (377)
HESX1 (47)
APOBEC3F (464.2)
CD274 (264)
CCND3 (350)
IFI30 (312)
MAX (359)
LYRM2 (482)
STAT2 (341)
SLC25A30 (353)
RPL22 (35)
DYNLT1 (186)
SPSB1 (205)
FKBP5 (233)
TNFSF13 (70.1)
CLEC2B (348)
FAM46A (333)
FAM46C (96)
IL18BP (420)
FLJ23556 (370)
IRF27 (347)
PARP9 (487)
BUB1 (180.1)
ZNF385B (305)
KCTD14 (544)
HIST2H2AA3 (519)
TIMP1 (557.1)
TRAFD1 (288)
RARRES3 (263.1)
CLDN23 (405.1)
CLDN23 (405)
NAPA (266)
TIMP1 (291)
ADFP (106)
FNDC4 (319)
SLCO5A1 (451)
LIPA (314)
SLC16A4 (457)
PHF11 (49)
HIST2H2AA4 (551)
SLC16A4 (457.1)
GBP1 (4)
GBP1 (4.2)
CCL7/C75 (11)
IFI44 (231)
IFNGR1 (118)
APOL2 (80)
XAF1 (211.2)
PSMB8 (2)
IFI6 (3)
RAB27A (198)
ARG2 (89)
IL1RN (290)
PPM1K (281)
XAF1 (211.1)
PLA2G4C (398)
VAMP5 (30)
C4orf33 (54)
ACSL5 (395.2)
XAF1 (211)
TMEM51 (67)
IFIT5 (116)
PXK (143)
PXK (143.1)
USP18 (222.1)
USP18 (222)
CCL2 (27)
CD58 (478.1)
MT1E (391.1)
C1orf38 (496)
SERPINB9 (277)
GPX2 (48)
ACSL5 (395)
BCL2L14 (78)
GBP1 (4.1)
SERPING1 (121)
CCL5 (22)
HIST1H3D (401)
IL15RA (320)
Mx1 (6)
ANKRD22 (50)
B2M (31)
IFITM3 (5.1)
NFIL3 (109)
HIST1H2BB (495)
IFITM1 (33)
RGS1 (196)
TNFAIP6 (68)
ETV6 (108)
DEFB1 (18)
CCL4 (23)
TSLP (599)
TNFSF18 (568)
RXFP1 (470)
CCDC92 (79)
CXCL10 (25)
AKT3 (334)
C14orf83 (459)
ENPP2 (396.2)
PRKD2 (342)
PSME2 (458)
COMMD3 (51)
TNFSF10 (69)
TNFSF10 (69.1)
PAK3 (137)
ATF3 (193)
SAMD4A (304)
USP18 (527.3)
STAT1 (338)
BRDG1 (582)
VIPERIN (388)
JUNB (362)
UBE2L6 (189)
TNFSF13B (70)
BTN3A2 (507.1)
BTN3A2 (507)
IFI16 (161.1)
IFI16 (161)
TRIM38 (235)
MT1E (391.2)
LGALS9 (212)
ZAP (389)
TLK2 (164.1)
TLK2 (164)
TNFRSF10A (111)
SAMD9 (477)
FNDC3B (311)
CEACAM1 (133)
TMEM62 (449)
OASL (126)
GSDMDC1 (411)
TRIM22 (450)
TYMP (117)
IRF2 (296.1)
NEXN (554)
XRN (572)
PNPT1 (254.1)
XRN (572.1)
MLH3 (473)
FLJ31033 (506)
DDX3X (250)
ZNF295 (324)
OGFR (384)
BTN3A3 (146.1)
IRF2 (296)
DCP1A (145)
IFI35 (208)
C3AR1 (426)
SLC1A1 (132)
PARP12 (159)
PLEKHA4 (168.1)
PLEKHA4 (168)
CASP1 (357)
SAMD9L (480)
RHOB (466)
PIM3 (213)
HERC5 (513)
DHX58 (157)
EIF2AK2 (10)
IL4I1 (486)
TNFSF14 (249.1)
PABPC4 (249)
C9orf52 (423)
C5orf39 (294)
SAT1 (44)
ADAMDEC1 (367.2)
APOBEC3G (95)
APOBEC3B (529)
APOBEC3F (464)
APOBEC3F (464.1)
MLKL (403)
SLFN12 (144)
UNC93B1 (307)
APOBEC3B (529.1)
MOV10 (177)
BST2/THN (45)
BST2/THN (45.1)
CDKN1A (191)
IDO1 (97)
TMEM140 (46)
CCNA1 (297.1)
MAP2 (424)
CTSS (514)
ETV7 (82)
LDB1 (494.1)
FBXO6 (73)
ELF1 (246)
HPSE (136.1)
IFITM3 (5)
IRF1 (270)
MYD88 (268)
TRIM5-5 (240.4)
TRIM5-4 (240.3)
TRIMCYP (240.5)
TRIM5-3 (240.2)
TRIM5-2 (240.1)
TRIM5-1 (240)
IFNB1 (465)
BCL3 (284)
MKX (88)
*
*

Figure S3

Figure S3. Heat map representing effects of macaque ISGs on retroviral infection (Related to Figure 1 and Figure 2). The effect of ISGs in the 25 incoming and outgoing screens represented in a heat map. All screens were normalised to the screen average (100 arbitrary units) with inhibition indicated in red and enhancement in green. Absent data, due to inefficient transduction, is indicated in grey (ND). Where allelic variants, spliced variants and repeated genes occur in the library, all data is presented and represent separate values from distinct transduction/transfection events. Asterisks denote clusters of ISGs whose protective effect is most evident in THP-1 cells. Heatmaps were produced using Gitools 2.2 and genes were hierarchically clustered using Manhattan maximum distance.

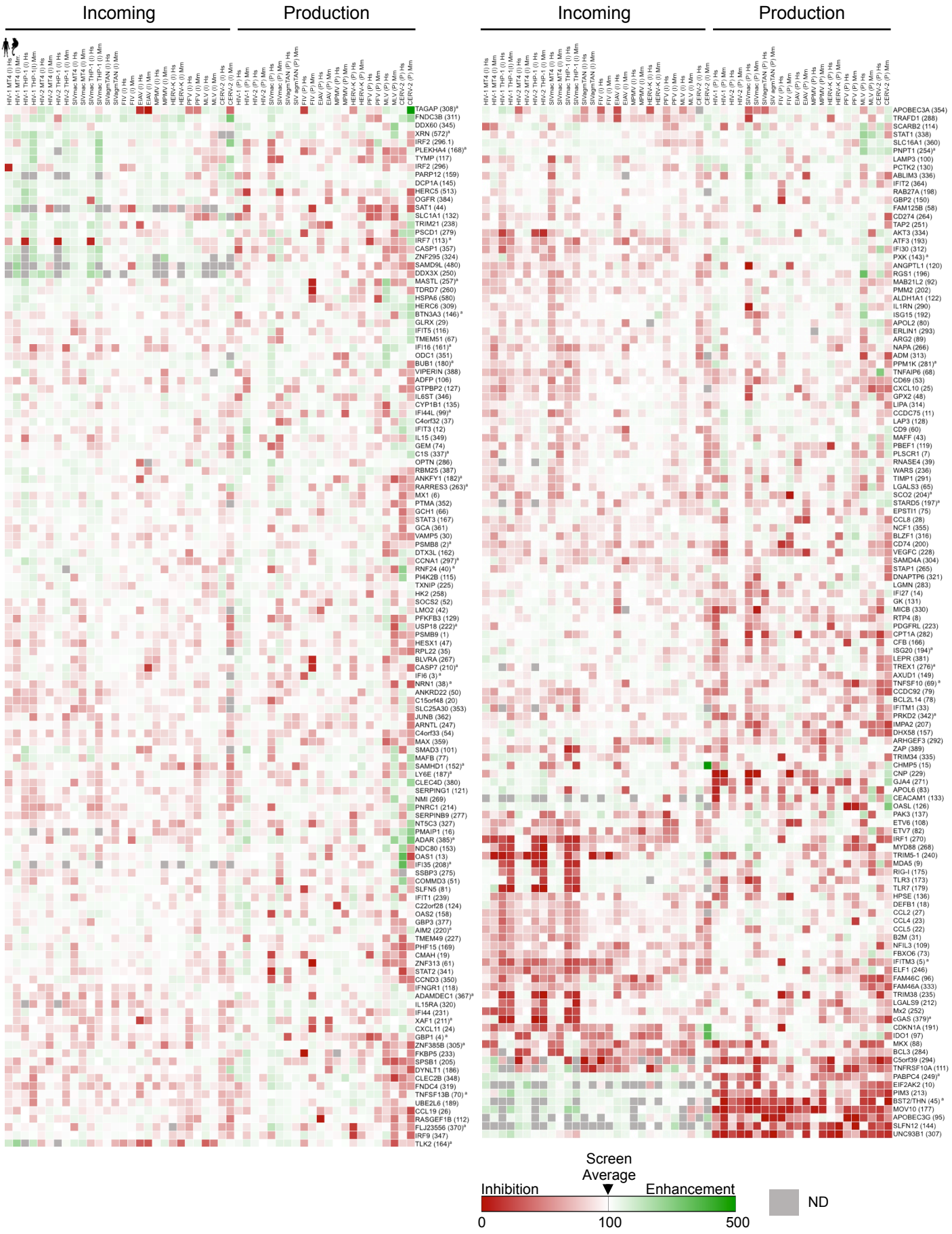
Incoming
Production
Incoming
Production
Screen Average
Inhibition
Enhancement
0
100
500
ND

Figure S4

Figure S4. Heat map comparing effects of human and macaque ISGs on retroviral infection (Related to Figure 1 and Figure 2). The effect of ISGs present in both human and macaque libraries in the 25 incoming and outgoing screens represented in a heat map (human left, macaque right for each screen). All screens were normalised to the screen average (100 arbitrary units) with inhibition indicated in red and enhancement in green. Absent data, due to inefficient transduction, is indicated in grey (ND). Where allelic variants, spliced variants and repeated genes occur in the library, all data is presented and represent separate values from distinct transduction/transfection events. Heatmaps were produced using Gitools 2.2 and genes were hierarchically clustered using Manhattan maximum distance.

[a] Multiple library copies (PSMB8, IFI16, GBP1, NRN1, RNF24, THN, TNFSF10, TNFSF13B, IRF7, HSPE, PXK, BTN3A3, SAMHD1, IFI16, PLEKHA4, MOV10, BUB1, IFI44L, ANKFY1, LY6E, ISG20, STARD5, SCO2, AIM2, IFI35, CASP7, XAF1, USP18, PABPC4, RARRES3, PNPT1, MASTL, TREX1, PPM1K, CCNA1, TAGAP, PRKD2, C1S, ADAMDEC1, FLJ23556, cGAS, ADAR, XRN)

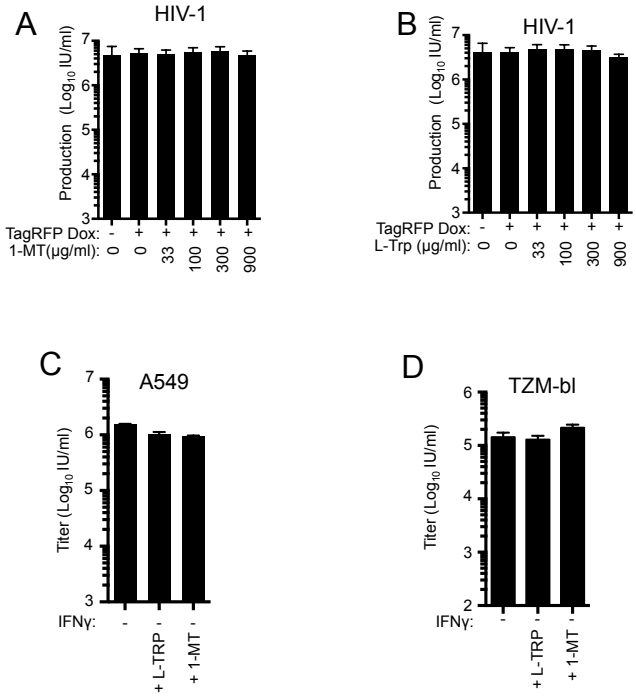
A
HIV-1
Production (Log10 IU/ml)
TagRFP Dox: - + + + + +
1-MT(μg/ml): 0 0 33 100 300 900
B
HIV-1
Production (Log10 IU/ml)
TagRFP Dox: - + + + + +
L-Trp (μg/ml): 0 0 33 100 300 900
C
A549
Titer (Log10 IU/ml)
IFNγ: - - + L-TRP - + 1-MT
D
TZM-bl
Titer (Log10 IU/ml)
IFNγ: - - + L-TRP - + 1-MT

Figure S5

Figure S5. 1MT and L-Trp do not affect HIV-1 replication without IDO1 induction or IFNγ treatment (Related to Figure 4 and Figure 5).

(A, B) Effects of 1-MT (A) or L-Trp (B) on the yield of infectious HIV-1 particles during a single cycle of HIV-1 replication in control MT4 cells (containing doxycycline inducible TagRFP)

(C) The yield of infectious progeny virions from a single cycle of HIV-1 replication in A549 cells without IFN-γ treatment in the presence of 50 μg/ml L-Trp or 100 μg/ml 1-MT

(D) As in C with TZM-bl cells, using 33 μg/ml L-Trp (TZM-bl cells) or 100 μg/ml 1-MT. Titers are mean+SD

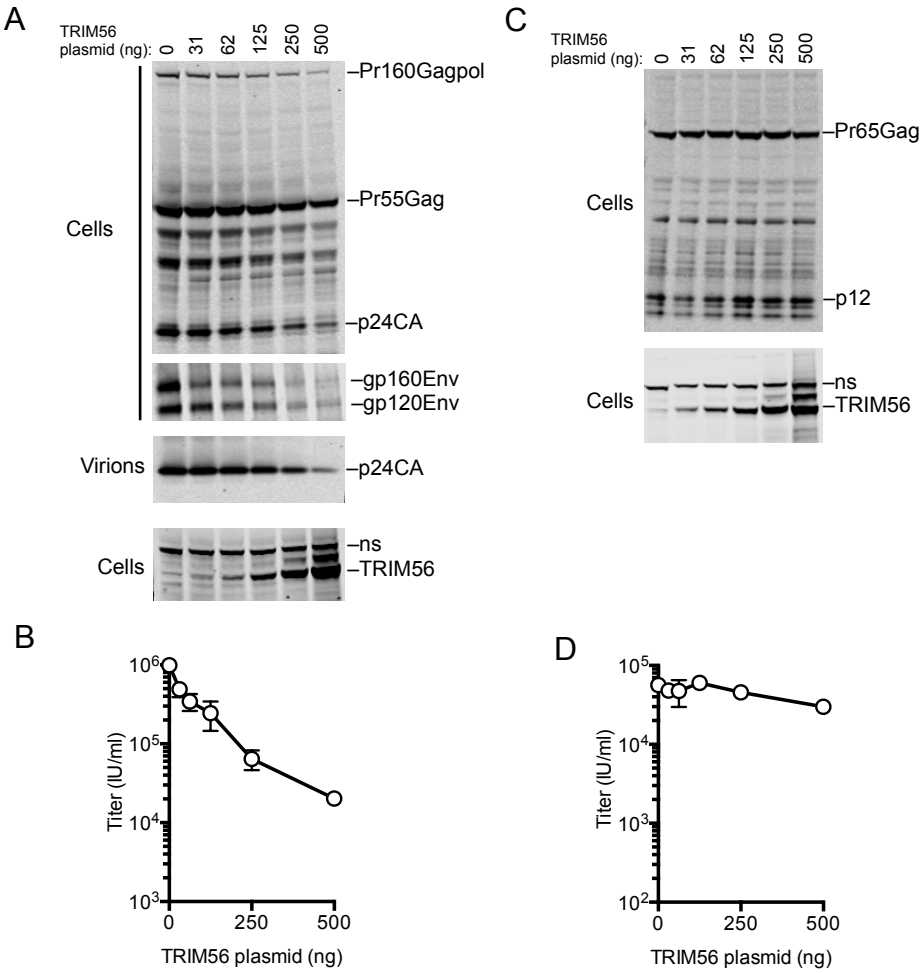
A
TRIM56
plasmid (ng):
0
31
62
125
250
500
Pr160Gagpol
Pr55Gag
p24CA
Cells
gp160Env
gp120Env
Virions
p24CA
Cells
ns
TRIM56
C
TRIM56
plasmid (ng):
0
31
62
125
250
500
Pr65Gag
Cells
p12
Cells
ns
TRIM56
E
Virion p24 (a.u.)
6
5
4
3
0.5
0.25
B
Titer (IU/ml)
10^6
10^5
10^4
10^3
0
250
500
TRIM56 plasmid (ng)
D
Titer (IU/ml)
10^5
10^4
10^3
10^2
0
250
500
TRIM56 plasmid (ng)

Figure S6

Figure S6. Effects of TRIM56 on HIV-1 replication (Related to Figure 6).
(A) Western blot analysis of HIV-1 Gag, Env and TRIM56 expression and particle release following transient cotransfection of 293T cells with HIV-1 proviral plasmids and increasing amounts of a TRIM56 expression plasmid.
(B) Western blot analysis of MLV Gag and TRIM56 expression and particle release following transient cotransfection of 293T cells with MLV GagPol and vector plasmids, along with VSV-G and increasing amounts of a TRIM56 expression plasmid.
(C) The yield of infectious HIV-1 virions from cells transfected in panel (A).
(D) The yield of infectious MLV virions from cells transfected in panel (B).
(E) Quantitation of virion associated p24 CA generated in a single cycle of infection of GHOSTX4 and GHOSTX4-TRIM56 cells. Titers are mean+SD

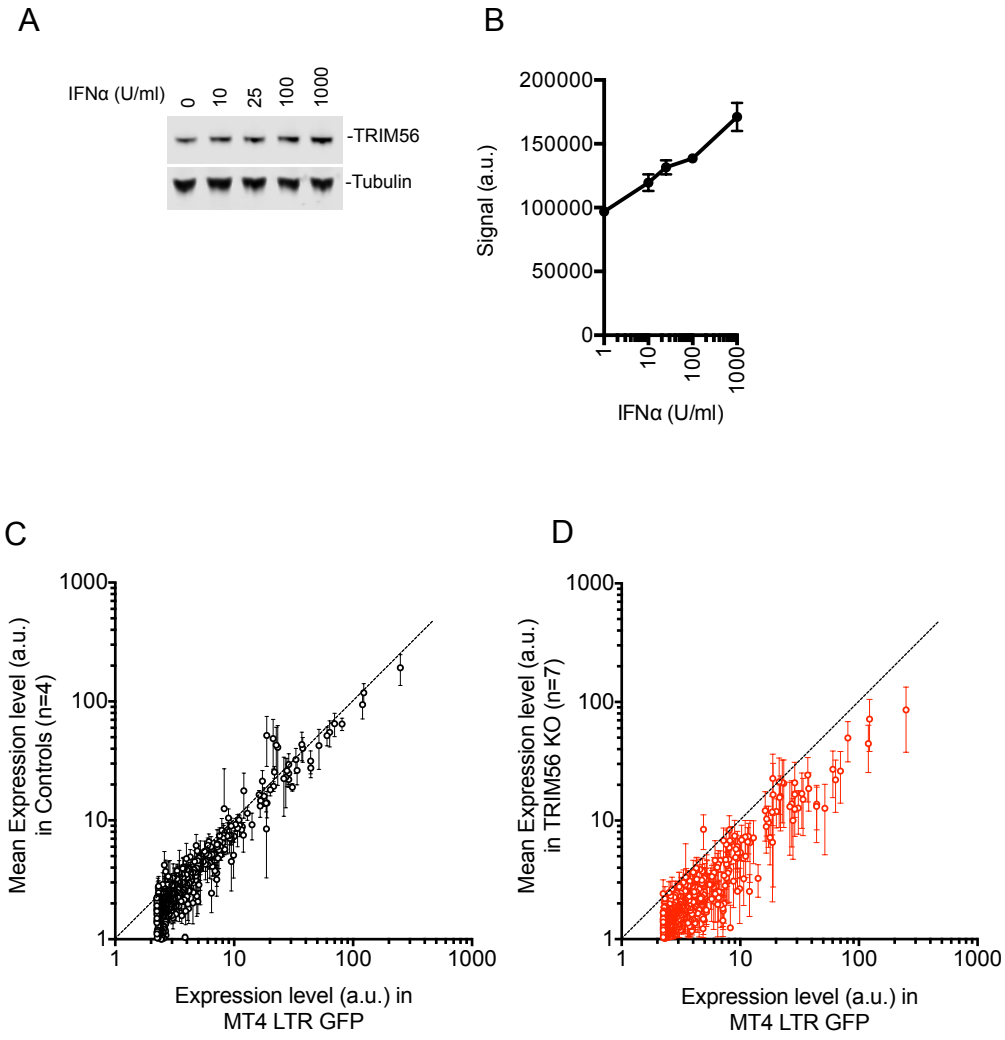
A
IFNα (U/ml)
0
10
25
100
1000
-TRIM56
-Tubulin
B
Signal (a.u.)
200000
150000
100000
50000
0
1
10
100
1000
IFNα (U/ml)
C
Mean Expression level (a.u.) in Controls (n=4)
Expression level (a.u.) in MT4 LTR GFP
D
Mean Expression level (a.u.) in TRIM56 KO (n=7)
Expression level (a.u.) in MT4 LTR GFP

Figure S7

Figure S7. Induction of TRIM56 and ISG expression by IFNα (Related to Figure 7).
(A, B) Western blot analysis of TRIM56 protein levels in MT4-LTR-GFP cells treated with increasing doses of IFNα. A typical blot (A) and quantitiation (B) is shown (B, mean ± SD).
(C, D) Microarray analysis of the expression levels (in arbitrary units, a.u.) of 500 genes induced by 25U/ml IFNα in unmodifed MT4-LTR-GFP cells (X-axis) versus corresponding mean values (Y-axis) for clones of control (C, mean ± SD n=4) or TRIM56-knockout (D, mean ± SD, n=7) MT4-LTR-GFP cells. The diagonal dashed lines indicate positions on which data points would fall if values were equivalent in the two plotted datasets.

Table S1. Viral plasmids and target cells for ISG screens (Related to Figures 1 and 2)

			Target cells	
Virus	**Plasmid(s)**	**Reference(s)**	**Incoming screens**	**Outgoing[a] Screens**
HIV-1	pNHG (JQ585717)/VSV-G	(Wilson et al., 2012)	MT4, THP-1	n/a
	pNL4.3 (M19921)	(Adachi et al., 1986)	n/a	MT4-TMZ[b]
HIV-2	Δ*nef*Δ*env* EGFP/VSV-G	(Hatziioannou et al., 2003)	MT4, THP-1	MT4
SIVmac	Δ*nef*Δ*env* EGFP/VSV-G	(Hatziioannou et al., 2003)	MT4, THP-1	MT4
SIVagmTAN	Δ*nef*Δ*env* EGFP/VSV-G	(Hatziioannou et al., 2003)	MT4	MT4
FIV	Gag-Pol/packageable genome /VSV-G	(Kemler et al., 2002)	MT4	MT4
EIAV	Gag-Pol/packageable genome /VSV-G	(Mitrophanous et al., 1999)	CRFK	MT4
MPMV	pSARM-EGFP/VSV-G	(Newman et al., 2006)	MT4	MT4
HERV-K	Gag-Pol/K-rec/packageable genome /VSV-G	(Lee and Bieniasz, 2007)	MT4	293T
MLV	Gag-Pol/packageable genome /VSV-G	(Soneoka et al., 1995) (Neil et al., 2001)	MT4	MT4
CERV-2/MLV	CERV2/MLV chimeric Gag-Pol/packageable genome /CERV2-Env	(Perez-Caballero et al., 2008; Soll et al., 2010)	293T	293T
PFV[a]	Δ*bet*Δ*bel3* 2A-EGFP	(Bock et al., 1998; Schmidt and Rethwilm, 1995)	HT1080	HT1080

[a] HEK 293T cells were used as producer cells for all outgoing screens with the exception of PFV, in which HT1080s were used.
[b] MT4 TMZ cells are a single cell clone derived from MT4 cells that encode an HIV-1 LTR-GFP reporter construct [T.M. Zang and P.D. Bieniasz, unpublished data and (Busnadiego et al., 2014)]

Table S2. ISG-encoding vectors with low titer (Related to Figures 1 and 3)

SPECIES	ISG	Antiretroviral? [b]	TRANSDUCTION (MT4)[a]	TRANSDUCTION (THP-1)[a]
Human	MDA5	IFN hit	44.10	13.32
Human	EIF2AK2	YES	27.15	2.19
Human	IFITM1	No	71.05	6.85
Human	RNASE4	No	113.75	8.97
Human	RNF24	No	90.62	19.45
Human	SAT1	No	7.71	1.06
Human	BST2/THN	YES	64.18	2.52
Human	FLJ11286	No	92.52	15.81
Human	APOBEC3G	YES	0.36	0.66
Human	TNFRSF10A	IFN Hit	29.82	2.98
Human	CEACAM1	YES	1.06	0.26
Human	FUT4	No	104.85	15.74
Human	SLFN12	YES	0.97	0.55
Human	DCP1A	No	91.00	14.00
Human	PARP12	No	66.09	4.24
Human	TLK2	YES	56.61	4.60
Human	TRIM56	YES	14.48	12.29
Human	PLEKHA4	No	105.49	11.93
Human	MAP3K14	IFN hit	98.12	3.82
Human	MOV10	YES	5.84	1.83
Human	NOS2A	YES	4.56	1.02
Human	STARD5	No	112.73	8.15
Human	FFAR2	YES	64.95	16.88
Human	DDX3X	No	1.26	3.29
Human	IRF1	IFN hit	96.08	12.50
Human	TREX1	YES	89.86	9.10
Human	BCL3	YES	107.01	9.35
Human	C5orf39	YES	10.88	13.03
Human	UNC93B1	YES	85.79	11.98
Human	IL15RA	No	100.40	8.44
Human	ZNF295	No	19.38	3.36
Human	CASP1	No	27.91	7.35
Human	ADAMDEC1	YES	103.71	18.36
Human	OAS3	YES	20.47	3.39
Human	ABCA9	No	22.80	0.44
Human	SAMD9L	No	0.60	2.14
Human	PARP10	No	36.86	5.24
Human	HERC5	No	99.01	13.15
Human	TGFB1	IFN hit	103.58	19.06
Human	TNK2	YES	61.26	7.06
Macaque	EIF2AK2	YES	0.08	0.39
Macaque	PMAIP1	No	61.49	2.23
Macaque	RNF24	No	84.49	10.76
Macaque	RNF24[c]	No	74.24	4.16
Macaque	SAT1	No	10.71	0.95
Macaque	BST2/THN	YES	1.07	0.85
Macaque	BST2/THN[c]	YES	1.35	2.27
Macaque	APOBEC3G	YES	63.62	17.99
Macaque	TNFRSF10A	IFN Hit	20.51	1.97
Macaque	IRF7	IFN Hit	101.11	12.11
Macaque	IRF7[c]	IFN Hit	93.61	3.73
Macaque	IRF7[c]	IFN Hit	85.11	1.20
Macaque	CEACAM1	YES	60.74	3.96
Macaque	SLFN12 (isoform 2)	YES	0.85	1.31
Macaque	PARP12	No	85.36	5.61
Macaque	TLK2	YES	22.75	12.77
Macaque	MOV10	YES	18.57	16.15
Macaque	ISG20	No	64.62	9.89
Macaque	IFI35	No	6.47	0.66
Macaque	DDX3X	No	14.75	20.33
Macaque	C5orf39	YES	3.25	5.73
Macaque	UNC93B1	YES	100.11	12.26
Macaque	ZNF295	No	30.93	11.61
Macaque	C6orf150	YES	84.61	10.75
Macaque	MLKL	YES	8.92	0.23
Macaque	APOBEC3F	YES	29.42	0.84
Macaque	APOBEC3F[c]	YES	39.49	0.70
Macaque	RHOB	No	3.18	3.91
Macaque	SAMD9L	YES	3.32	63.70
Macaque	BTN3A1	YES	2.48	0.60
Macaque	APOBEC3B	No	5.18	14.73

[a] Normalized transduction (% of screen average)
[b] Stimulated IFNβ/ISRE driven reporter activity (IFN hit), Appears (yes) or does not appear (No) in Table S1 (ISGs with antiretroviral activity)
[c] Multiple library copies (RNF24, THN, IRF7, APOBEC3F)

Table S3. Human ISGs subtracted due to ISRE or IFNβ promoter stimulation (Related to Figure 3)

ISG	IFNβ 293T[a]	IFNβ THP1[a]	ISRE 293T[a]
EPSTI1	9.87	1.59	0.50
IL1R	0.73	24.71	0.65
IRF1	11.41	1.33	74.83
IRF7	1.40	0.91	65.14
MAFF	0.68	1.46	6.83
MAP3K14	365.11	39.42	49.44
MAP3K5	1.72	34.32	0.20
MDA5	10.88	1.16	51.38
MYD88	192.01	44.87	1.75
NOD2	22.38	6.88	0.55
P2RY6	6.04	1.88	3.02
RIG-I	3.80	1.12	6.12
RIPK2	85.93	36.50	0.68
RIPK2[b]	112.12	140.93	1.15
TBX3	1.59	0.71	7.02
TGFB1	21.40	1.25	0.69
TLR7	0.64	15.66	1.74
TNFRSF10A	243.76	0.63	3.22
TRIM25	43.36	85.06	0.06
TRIM38	12.16	12.37	0.85

[a] Fold-activation of reporter gene expression
[b] Two library copies (RIPK2)

Table S4. Macaque ISGs subtracted due to ISRE or IFNβ promoter stimulation (Related to Figure 3)

ISG	IFNβ 293T[a]	IFNβ THP1[a]	ISRE 293T[a]
AIM2	0.92	22.92	1.06
AIM2[b]	1.31	15.62	0.98
IFI16	0.81	8.83	0.38
IFNB1	0.75	1.31	62.74
IRF1	11.56	0.85	63.34
IRF7	2.24	9.49	29.32
IRF7[b]	2.85	20.08	14.72
MYD88	11.09	17.13	1.24
PRKD2	0.99	7.39	0.46
RIG-I	10.58	0.40	4.25
TNFRSF10A	28.80	0.63	5.64
TRIM38	1.27	14.34	0.98
TRIM5-5	1.17	7.88	1.06

[a] Fold-activation of reporter gene expression
[b] Two library copies (AIM2 and IRF7)

Table S5. ISGs with anti-retroviral activity (Related to Figure 1, Figure 2, and Figure S1).

ISG[a]	Incoming Screens (Hs)[b]	Incoming Screens (Mm)[b]	Production Screens (Hs)[c]	Production Screens (Mm)[c]	Anti-SCRPSY[d]	Reported anti-retroviral activity[e]	Reference(s)
IDO1	HIV-2(MT4)	HIV-2(MT4)				Here	
TRIM56			HIV-1, HERV-K		Yes	Here	
ADAMDEC1				HIV-1, SIVagmTAN, PFV	Yes	No	
AKT3	HIV-1(THP-1), HIV-2(THP-1)	HIV-2(THP-1)				No	
ANGPTL1			SIVmac			No	
APOBEC3A	EIAV, HERV-K					Yes	(Berger et al., 2011)
APOBEC3B				HIV-1, HIV-2, SIVmac, PFV SIVagmTAN, MLV, CERV-2		Yes	(Yu et al., 2004)
APOBEC3F				HIV-1, SIVagmTAN, PFV	Yes	Yes	(Wiegand et al., 2004)
APOBEC3G			SIVagmTAN, FIV, PFV	SIVagmTAN, PFV, HIV-1	Yes	Yes	(Sheehy et al., 2002)
APOL1			FIV			Yes	(McLaren et al., 2015; Taylor et al., 2014)
APOL6	SIV(THP-1)	EIAV	HIV-1, MPMV			Yes	(McLaren et al., 2015)
B4GALT5			EIAV			No	
BCL3	HIV-2(MT4), SIVmac(MT4), FIV	HIV-2(MT4), SIVmac(MT4), FIV			Yes	Yes	(Hishiki et al., 2007)
BIRC3			FIV			No	
BLVRA				FIV		No	
BST2/THN[f]			SIVmac, MLV	SIVmac, MLV, HIV-1, FIV, EIAV, MPMV, CERV-2	Yes	Yes	(Neil et al., 2008)
BTN3A1				CERV-2	Yes	No	
C17orf60				MPMV		No	
C22orf28			MPMV			No	
C5orf39	HIV-2(MT4), SIVmac(THP-1), FIV		HERV-K, CERV-2	HIV-1, SIVmac	Yes	No	
C9orf52				HERV-K		No	
CASP7		EIAV	FIV			No	
CCR1			FIV, EIAV, HERV-K			No	
CD163			HERV-K			No	
CD74			FIV			Yes	(Schoggins et al., 2015)
CDKN1A		HIV-1(MT4), HIV-2(THP-1)	FIV			Yes	(Pauls et al., 2014)
CEACAM1			HIV-1		Yes	No	
CEBPD			SIVmac			No	
cGAS	SIVmac(THP-1), HIV-1(THP-1), HIV-2(THP-1)	SIVmac(THP-1), HIV-1(THP-1), HIV-2(THP-1)			Yes	PI	(Gao et al., 2013; Schoggins et al., 2014; Schoggins et al., 2015)
CHMP5	SIVmac(THP-1)					Yes	(Kuang et al., 2011; Pincetic et al., 2010)
CLEC2B				MLV		No	
CLEC4A	SIVmac(MT4)					No	
CNP			HIV-1, SIVmac	HIV-1, SIVmac, FIV		Yes	(Wilson et al., 2012)
CPT1A			SIVmac, EIAV, CERV-2			No	
CRY1			FIV			No	
CX3CL1			HIV-1, EIAV			No	
EHD4			HIV-1, EIAV			No	(Bregnard et al., 2013)
EIF2AK2				SIVmac	Yes	PI, Yes	(Deb et al., 2001; Yoon et al., 2015)
ELF1	SIVmac(THP-1)	HIV-2(MT4)				No	(Leiden et al., 1992)
ENPP2				FIV		No	
EPAS1	EIAV		HERV-K			No	
ETV7		MPMV				No	
EXT1			SIVmac, HERV-K, CERV-2			No	
FAM46A	MPMV					No	
FAM46C	HIV-1(THP-1), HIV-2(THP-1), HERV-K					No	(Telenti and Johnson, 2012)

FFAR2			HIV-1, HIV-2, SIVmac, SIVagmTAN, FIV, EIAV, MPMV, HERV-K, PFV, MLV, CERV-2		Yes	No	
FKBP5			FIV			No	
FLJ23556			HERV-K			No	
FOXN2				FIV		No	
GAK			MPMV			No	
GALNT2			HIV-1, SIVmac, FIV, CERV-2			No	
GBP2			FIV			No	
GJA4			HIV-1, SIVmac			No	
GPR37				HIV-1, SIVmac		No	
HIST1H3D				SIVmac		No	
HPSE				FIV		No	
MDA5		HIV-1(THP-1), HIV-2(THP-1), SIVmac(THP-1)				PI	(Andrejeva et al., 2004)
IFITM3	SIVmac(THP-1), HIV-1(THP-1)	SIVmac(THP-1), HIV-1(THP-1)	FIV			Yes	(Brass et al., 2009; Compton et al., 2014)
IL1RN			SIVmac			No	
IL4I1				SIVmac		No	
IRF2	HIV-1(MT4)					No	
IRF9			HERV-K			PI	(Randall and Goodbourn, 2008)
LAMP3	SIVmac(MT4)					No	
LDB1				EIAV		No	
LGALS9		HIV-2(THP1), SIVmac(THP-1)				PI	(Matsuura et al., 2009)
MACS			HIV-1			No	
MASTL				FIV		No	
MICB				SIVmac		No	
MKX	EIAV		HIV-1, SIVagmTAN			No	
MLKL				HIV-1, HERV-K, CERV-2, PFV	Yes	No	
MOV10			HIV-1, SIVmac, SIVagmTAN, FIV, MPMV, PFV, CERV-2	HIV-1, SIVmac, SIVagmTAN, FIV, MPMV	Yes	Yes	(Furtak et al., 2010; Wang et al., 2010)
Mx2	HIV-1(THP-1), HIV-2(THP-1), SIVmac(THP-1)	HIV-1(MT4), SIVmac(THP-1)				Yes	(Goujon et al., 2013; Kane et al., 2013; Liu et al., 2013)
NFIL3	SIVmac(THP-1)					No	
NOS2A	HIV-2(MT4)		HERV-K, CERV-2		Yes	No	
OAS3			CERV-2		Yes	No	
OASL			PFV	PFV		No	
PABPC4				HIV-1, SIVmac		No	
PAK3	PFV					No	(Nguyen et al., 2006)
PBEF1			HERV-K			No	
PIM3				HIV-1, CERV-2		No	
PPM1K				FIV		No	
PRAP1				SIVagmTAN		No	
RASGEF1B			EIAV			No	
RHOB				HIV-1	Yes	PI	(Xu et al., 2014)
RNF19B			HIV-1			No	
SAMD9		HIV-2(MT4)		FIV		No	
SCO2				FIV		No	
SLC15A3			HIV-1, SIVmac, MPMV, CERV-2			PI	(Nakamura et al., 2014)
SLC16A4		HIV-1(THP-1)				No	
SLC2A12				FIV		No	
SLFN12			HERV-K	HIV-1, HIV-2, SIVmac, HERV-K, EIAV, CERV-2, PFV	Yes	No	
SP100	SIVmac(THP-1)					No	
SQLE			FIV			No	
STAT2			SIVmac			PI	(Randall and Goodbourn, 2008)
TAGAP	EIAV	EIAV		SIVmac		No	
TDRD7				FIV		Yes	(Lu et al., 2011)
THBD			HIV-1			No	

TLK2		EIAV			Yes	No	
TLR1		HIV-2(THP-1)				PI	(Pasare and Medzhitov, 2005)
TLR3	SIVmac(THP-1)	HIV-1(THP-1), HIV-2(THP-1), SIVmac(THP-1)	SIVmac			PI	(Gibbert et al., 2014; Pasare and Medzhitov, 2005)
TLR7		HIV-1(THP-1), HIV-2(THP-1), SIVmac(THP-1)				PI	(Kane et al., 2011; Pasare and Medzhitov, 2005)
TMEM173		SIVmac(THP-1)				PI	(Burdette et al., 2011)
TNFSF10[f]				PFV		No	
TNK2			HIV-1		Yes	No	
TRAFD1	EIAV					No	
TREX1				SIVmac	Yes	No	(Yan et al., 2010)
TRIM34			FIV			Yes	(Zhang et al., 2006)
TRIM5[f]	HIV-1(THP-1), HIV-2(THP-1), SIVmac(THP-1)	HIV-1(MT4,THP-1), HIV-2(MT4,THP-1), SIVmac(THP-1),SIVagmTAN, FIV				Yes	(Stremlau et al., 2004)
TRIMCYP		HIV-2(MT4, THP-1), FIV, SIVagmTAN		SIVmac		Yes	(Sayah et al., 2004; Wilson et al., 2008)
ULK4			FIV			No	
UNC84B (SUN2)	HIV-1(THP-1), HIV-2(THP-1)					Yes	(Donahue et al., 2016; Lahaye et al., 2016)
UNC93B1			HIV-1, SIVmac, SIVagmTAN, HERV-K, MLV, CERV-2	HIV-1, HIV-2, SIVagmTAN, HERV-K, MLV, CERV-2, EIAV, MPMV	Yes	PI	(Kim et al., 2008)
USP18				SIVmac		No	
XAF1	EIAV					No	
ZC3HAV1	SIVmac(THP-1)	SIVmac(THP-1)				Yes	(Gao et al., 2002)
ZNF107			SIVagmTAN			No	
ZNF313				FIV		No	

[a] ISGs which stimulated the IFNβ or IRSE promoter (Figure 3 and Table S3 and S4) are subtracted from this list. Hyperlinks are to the UniProt entries of the human orthologue (not necessarily the isoform screened).

[b] Viruses inhibited by 3-fold or greater in incoming screens, cell type indicated in parenthesis for cases in which ISGs were tested in more than one screen.

[c] Viruses inhibited by 5-fold or greater in production screens.

[d] ISGs that affected titer/transduction of the SCRPSY vector (Figure S1 and Table S2) are indicated by “Yes”

[e] “PI” indicates genes reported to have pro-inflammatory activity such as activating anti-viral cytokine production/signaling

[f] Multiple library copies (TNFSF10, THN, TRIM5, PABPC4, TAGAP, APOBEC3F, APOBEC3B)

Extended Experimental Procedures

Cell lines

The feline CRFK cells, macaque FRhK4 and LLC-MK2 and adherent human HEK 293T, TE671 and TZM-bl cell lines were maintained in Dulbecco's Modified Eagle's Medium (DMEM) with 10% FBS and gentamicin. GHOSTX4 (a single cell clone of the original GHOSTX4R5 cell line obtained through the AIDS Reagent Program, Division of AIDS, NIAID, NIH from Dr. Vineet N. KewalRamani and Dr. Dan R. Littman) were maintained in DMEM supplemented with 2.5μg/ml puromycin, 50μg/ml hygromycin, and 500μg/ml G418. A549 cells were maintained in Ham's F12/DMEM, all supplemented with 9% fetal bovine serum (FBS) and gentamicin. Suspension rhesus 221 cells (RPMI supplemented with IL-2 and 17% FBS) and human MT4 and THP-1 cells were maintained in RPMI supplemented with 10% FBS and gentamicin. MT4-LTR-GFP indicator cells were generated by transduction with a lentivirus derived from pSIR LTR-GFP, a self-inactivating MLV reporter construct containing a cassette in which hrGFP expression is driven by the HIV-1 LTR. A single cell clone was generated by limiting dilution and maintained in 2.5μg/ml puromycin. ISG-expressing MT4 and GHOSTX4 cell lines were modified using lentiviral vectors. Limiting dilution was also used to generate a panel of GHOSTX4 cells, modified to express TRIM56. IFNβ1/ISRE reporter cell lines represent cell clones modified using MLV-derived retroviral vectors.

Retroviruses

Replication competent proviral clones encoding GFP (PFV) or VSV-G-pseudotyped envelope minus derivatives of HIV-1 (NHG Δ*env*/VSV-G), HIV-2 (HIV-2 Δ*env* EGFP/VSV-G), SIVmac (SIVmac Δ*nef* Δ*env* EGFP/VSV-G) and SIVagmTAN (Δ*nef* Δ*env* EGFP/VSV-G) or multi-plasmid VSV-G pseudotyped vector systems FIV, EIAV, HERV-K, and MLV were used as described previously (Busnadiego et al., 2014; Kane et al., 2013; Wilson et al., 2012). The 'CERV2' virus was generated using a chimeric construct containing a full length CERV2 Gag gene that is a consensus of endogenous CERV2 Gag sequences found in the chimpanzee genome (Perez-Caballero et al., 2008), linked to an MLV Pol sequence. CERV2 virions generated by co-transfection of 5μg of chimeric CERV2/MLV Gag-Pol, 5μg of MLV packageable genome, and 5μg of CERV2 envelope (Soll et al., 2010). In follow up analyses, intact proviral clones for HIV-1 (NL4-3) (M19921) and HIV-2 (ROD10) or GFP-encoding HIV-1 pNHG (JQ585717) with GFP in place of *nef* were also used. Intact proviral clones were pseudotyped with VSV-G as indicated.

Construction of an ISG library from rhesus macaques

An HIV-1 based vector pSCRPSY-DEST used to express the ISGs was based on a previously described HIV-1 based vector, pV1/hrGFP (Zennou and Bieniasz, 2006). pSCRPSY-DEST (GenBank accession KT368137) consists of a minimal packageable HIV-1 genome containing all essential *cis*-acting sequences with Gateway att^R and *Sfi*I restriction sites inserted in place of Nef, and a TagRFP-2A-$Puro^R$ cassette inserted in place of a deleted fragment containing *gag, pol, vif and vpr* genes. The *vpu* and *env* genes are also deleted or inactivated. Thus, cells transduced with pSCRPSY-DEST express HIV-1 Tat and Rev and any cDNA inserted into the DEST sequences from completely spliced 'early' HIV-1 transcripts, while TagRFP and PAC ($Puro^R$) are expressed from a late, unspliced HIV-1 transcript PAC2ATagRFP where PAC and TagRFP proteins are separated by a FMDV 2A stop-start peptide. In pilot experiments this vector format minimized the number of cells that expressed the transduction marker (TagRFP) but did not express a gene inserted into the DEST sites (typically EGFP).

Using the same criteria used to select human ISGs (Dittmann et al., 2015; Schoggins et al., 2011), primer pairs were designed to amplify ~600 different macaque genes by RT-PCR. In order to target genuine orthologous transcripts, multiple primer pairs were designed based on transcript variants of the most significant BLAST match of the rhesus macaque (*M. mulatta*) genome using human reference sequence ISGs as probes. Directional *Sfi*I restriction sites and 4 additional nucleotides were appended to the forward *Sfi*I oligos (5'-CTCT***GGCC****GAGAG****GGCC***ATG-3') and the final 3 nucleotides of the *Sfi*I site provided Kozak consensus sequences for the macaque ISGs. The reverse oligo also contained 4 additional nucleotides (5'-TCTC***GGCC****AGAGA****GGCC***TTA-3') and were immediately followed by the reverse complement of the ISG stop codon (ochre/UAA in this example). Each oligo also contained ~25 nucleotides complementary to the macaque ISG target. In total 864 primer pairs were designed and subsequently synthesized by Operon. IFNα-stimulated (1000 units/ml) FRhK4, LL-CMK2 and 221 cells were used as a source of macaque RNA (*M. mulatta*) for cDNA synthesis (superscript III). Pooled RNA from cells stimulated for 4, 16 and 24 hours was used. Each gene was PCR amplified using Pfu polymerase and reactions that did not yield the expected amplicon were repeated using Taq polymerase. PCR amplicons were conventionally cloned into a Gateway® (Invitrogen) compatible entry vector modified to contain directional *sfi*I sites. ISGs were subsequently sequence verified (Genewiz). ISG ORFs were selected for the library that either matched the amino acid sequence of NCBI macaque entries or yielded at least two clones with identical amino acid sequences. Selected ORFs were subcloned into pSCRPSY-DEST and pcDNA-

DEST40 (Invitrogen) destination vectors using LR-clonase (Invitrogen). The previously described arrayed human ISG library (Schoggins et al., 2011) was extended to include a small number of highly IFNα-stimulated human ISGs based upon the initial criteria used previously (Schoggins et al., 2011) and our own microarray data (Kane et al., 2013; Neil et al., 2008). This extended human library (Dittmann et al., 2015) was similarly transferred into pSCRPSY and pcDNA-DEST40 using LR-clonase. Prior to screening, the identity of human and macaque ISGs was confirmed using restriction digest (all clones) and scatter sequencing of ~10% of the libraries.

Screening ISGs for antiretroviral activity

For incoming screens, ISG-encoding lentiviral vectors (SCRPSY) were generated by cotransfection of 293T cells using polyethyleneimine with 25ng HIV-1 Gag-Pol and 5ng VSV-G expression vectors, along with 250ng of each SCRPSY-based ISG expression vector in a 96-well plate format ($0.35x10^5$ cells/well). Thereafter, culture supernatants were used to transduce the relevant susceptible target cells (THP-1 cells were spinoculated for 1hr at 1600 rpm). Transduced ISG-expressing cells were challenged 48 hours later with a single dose of the GFP-encoding retroviruses or retroviral vectors using a MOI ~0.5. Cells were fixed 48h post-infection and the percentage of TagRFP+ and GFP+ cells determined by flow cytometry. In order to determine ISGs that inhibit SCRPSY production (Figure S1 and Table S4, S5), the fraction of ISG/TagRFP-expressing cells was expressed as a percentage of the mean value across all wells for the respective library (*H. sapiens* or *M. mulatta*) in the HIV-1 incoming screens.

For production screens, 293T cells were transfected in a 96 well format, using polyethyleneimine with 75ng of ISG expression plasmids (pcDNA-DEST40) along with 5ng VSV-G expression vector, and 70ng of plasmids that generated GFP-transducing retroviruses (HIV-1, HIV-2, SIVmac, and SIVagmTAN), or 5ng of VSV-G with 35ng of Gag-Pol expression plasmid and 35ng of packageable genome (EIAV, FIV, and MLV), or 35 ng of chimeric CERV2/MLV Gag-Pol, 35ng of packeagable genome, and 35ng of CERV2-Env, or 7ng VSV-G with 50ng packageable genome, 38ng Gag-Pol, and 19ng K-Rec expression plasmids (HERV-K). At 48h after transfection, supernatants were harvested and used to challenge either MT4 cells (HIV-1, HIV-2, SIVmac, SIVagmTAN, EIAV, FIV, and MLV) or 293T cells (HERV-K and CERV2). For the PFV production screen, HT1080 cells were transfected with 75ng of ISG expression plasmids and 75ng PFV expression plasmid. At 48h post-transfection, cells were lysed by multiple freeze-thaws and lysates were used to challenge HT1080 cells. All cells were fixed 48h post-infection and the percentage of GFP+ cells determined by flow cytometry (see also Table S1).

For each ISG, the fraction of infected, ISG/TagRFP-expressing cells (incoming screens) or the yield of infectious virions (production screens) was expressed as a percentage of the mean value across all wells for the respective library (*H. sapiens* or *M. mulatta*) in a given screen, except the MPMV incoming screen, in which values are expressed as the mean value across each plate.

IFNβ1 and ISRE reporter cell lines and expression screens therein

We amplified the ISRE-Luc fragment containing 5 repeats of a canonical ISRE (ISRE - TAGTTTCACTTTCCC) from a pISRE-Luc plasmid (Agilent technologies, PathDetect ISRE cis Reporting System) using primers containing *Bgl*II sites and inserted this cassette upstream of the CMV IE promoter of pQCXIN (Clontech), in which NeoR has been replaced with the blasticidin resistant gene, termed pQCXIB. The plasmid used to make the reporter cell (ISRE-GFP) was constructed by insertion of 5 copies of the ISRE followed by the EGFP coding region into the *Bgl*II site, upstream of the CMV IE promoter of pQCXIB. The IFN beta promoter (-125 to +22) was amplified from human genomic DNA using primer pairs containing *Kpn*I at the 5'-end and *Hind*III at the 3'-end, respectively, and subcloned into pGL2-Luc (Promega). The IFN beta-Luc fragment was then amplified using primers containing *Bgl*II and subcloned into pQCXIB. To construct the reporter cells, we transduced 293T or THP-1, with a low multiplicity of infection (less than 0.1). After selection with blasticidin, limiting dilution and expansion, single clones were measured for luciferase activity upon IFNα treatment (for ISRE-GFP). Single responsive clones were chosen for the screening assays.

THP-1 and HEK 293T cells containing an IFN β-promoter-driven luciferase reporter were transduced with ISG libraries and luciferase activity measured 48hrs later with Luciferase Assay System (Promega E1501) using Modulus™ II (Turner BioSystems). To reflect total IFN β-promoter induction, these screens were not normalized and fold change is presented. HEK 293T cells containing the ISRE-driven GFP reporter were transduced with human and macaque ISG libraries, mock treated or treated with 100 units/ml IFNα, and GFP+ and RFP+ cells enumerated 12 hours later using flow cytometry. To reflect ISRE activation per transduced cell, these ISRE screens were normalized. ISGs stimulating ISRE/IFNB1 driven reporter expression by >5 fold (normalized to SCRPSY transduction levels) were excluded from further examination of the candidate 'directly acting inhibitors' of incoming retroviral infection and are listed in Table S2 and S3.

Stable or inducible expression of individual ISGs for follow–up studies

For constitutive expression of ISGs in follow up studies, a lentiviral vector CCIB was derived from CSGW by replacing sequences encoding GFP with a multi-cloning site followed by an IRES sequence and a blasticidin resistance cassette. The SFFV promoter was also replaced with a CMV promoter. A selection of genes that inhibited HIV-1 NL4-3 by 3-fold or more during an outgoing library screen were cloned into CCIB using *Sfi*I, *Pme*I-*Not*I, *Xmn*I/*Pme*I-*Not*I, *Pme*I or *Not*I restriction site combinations. These genes included the human FFAR, SLC15A3, TRIM56, APOL6, TBX3, EHD4, MOV10, GJA4, UNC93B1, TNK2, CX3CL1, MKX, MARCK, EXT1, CEACAM1 and OAS3, and the macaque MLKL, SLFN12, GPR37, PABPC4, C5ORF39, RHOB, SAT1, MOV10, GJA4 and UNC93B1. GHOSTX4 cell lines expressing each of the aforementioned ISGs that exhibited anti-HIV-1 activity in outgoing screens were generated by transduction with CCIB based viruses followed by selection with 5μg/ml blasticidin. A control cell line containing empty vector CCIB was similarly generated. Multiple single-cell clones of GHOSTX4 expressing TRIM56 cells were derived by limiting dilution, and the continued expression of CD4 and CXCR4 was verified using flow cytometry.

For doxycycline-inducible expression of ISGs, the modified tetracycline-inducible lentiviral expression vectors (pLKOΔ-Myc-TRIM5α-IP, pLKOΔ-Myc-TagRFP-IP, pLKOΔ-Myc-TRIM5α-IN, pLKOΔ-Myc-TagRFP-IN) have been previously described (Busnadiego et al., 2014). HsIDO1 was amplified from the human ISG library and cloned into the same lentiviral expression vectors to produce pLKOΔ-Myc-IDO1-IP and pLKOΔ-Myc-IDO1-IN using directional *Sfi*I sites. Doxycycline-inducible cell lines were produced via transduction of MT4 cells with modified LKO-derived lentiviral vectors, and subsequent selection with puromycin (2 μg/ml, Sigma) or G418 (1 mg/ml, Promega) as previously described (Busnadiego et al., 2014). ISG expression was induced in these cell lines using doxycycline hyclate (125 ng/ml, Sigma) for 24 hours prior to viral challenge.

For further examination of the candidate 'directly acting inhibitors' of incoming retroviral infection, human and macaque ISGs that conferred >2-fold protection from HIV-1 or HIV-2 infection in any incoming screen were investigated for their ability to protect cells from incoming HIV. This ISG list was filtered to remove ISGs that activated ISRE/IFNB1 driven reporter expression by >5-fold. The remaining ISGs (Human ISGs AKT3, B2M, BCL3, C5orf39, CCDC109B, CCL2, CCL4, CCL5, CDKN1A, CEBPD, cGAS, DDIT4, DEFB1, EPAS1, FAM46C, FBXO6, HPSE, IDO1, IFI30, IFITM3, IL15, IRF2, LGALS9, MKX, MT1H, Mx2, NOS2A, SCARB2, SP100, TRIM5, TRIM56 and UNC84B in addition to macaque ISGs AKT3, BCL3, BRDG1, BTN3A2, BTN3A2, BUB1, C1orf38, cGAS, CCNA1, CDKN1A, CHMP5, ELF1, GMPR2, IFI16, MDA5, IFITM3, IDO1, LDB1, LGALS9, LY6E, MKX, MT1E , Mx2, NAPA, PAK3, SAMD9, SAT1, SLC16A4, TLR1, TLR3, TLR7, TMEM140, TNFSF13B, TNFSF18, TRIM5-1, TRIM5-2, TRIM5-3, TRIM5-4 and TRIMCYP) were considered further and ISGs that conferred > 2-fold protection in the follow up subscreen are displayed in Fig 3. Human APOBEC3A met the criteria but was not tested in the subscreen due to low transduction levels. Human C5orf39 and NOS2A were overtly toxic in MT4 cells and were not considered further in this context. We were unable to achieve efficient transduction of THP-1 cells using vectors encoding macaque SAT1 and this gene was not considered further in this context.

CRISPR-mediated TRIM56 knockout

A derivative of the HIV based retroviral vector lentiCRISPR Version 2 (Addgene, Plasmid #52961) was constructed by replacing the puromycin resistance gene with a blasticidin resistance gene. TRIM56 CRISPR knockout constructs were made by inserting targeted guide sequences via *Bsm*BI into the modified vector. The CRISPR guide sequences CR1 and CR3 were designed using the CRISPR design program available at http://crispr.mit.edu/ (CR1 targets TRIM56 bp171-191 CGAGTGCCGCGAGACAGTGCC; CR3 targets TRIM56 bp 183-203, CGACAGTGCCTGTGCCGCCCGA). MT4-LTR-GFP knockout cells were derived by transduction with lentiCRISPRV2 based viruses followed by selection with 5μg/ml blasticidin. Single-cell clones derived from populations of cells transduced with control, CR1 and CR3 vectors were derived by limiting dilution and screened for strongly reduced or absent TRIM56 expression by western blotting. None of the control subclones exhibited reduced or absent TRIM56 expression.

Single cycle replication assays

For the incoming, single-cycle infectivity assays in the MT4 cells lines with doxycycline-induced IDO1, TRIM5α, or TagRFP expression and all titration experiments to determine infectious units in MT4 or MT4-LTR-GFP cells, cells were treated or not treated with doxycycline hyclate for 24h before viral challenge. At 16h post-infection, dextran sulfate was added to the HIV-1 (NHG) infected cells to limit infection to a single cycle. Cells were fixed 48h post-infection and the percentage of GFP+ cells determined by flow cytometry.

For viral production assays, MT4 cell lines were treated or untreated for 24h with doxycycline hyclate before infection with HIV-1 (NHG or NL4-3) using a MOI of ~0.3 or HIV-2 (VSV-G pseudotyped ROD10) using an MOI of ~0.6. Cells were also treated with L-tryptophan (Melford) or 1-methyl-L-tryptophan (1-MT, Sigma-Aldrich) at the time of infection, as indicated. At 44h post-infection, cells were lysed in SDS sample buffer and virus-containing

supernatant was harvested and filtered (0.22 um), before being titrated onto MT4 cells, in the case of NHG or TZM-bl cells in the case of HIV-1 NL4-3 and HIV-2.

For single cycle replication assays in A549/TZM-bl cells, cells were seeded in 6-well plates and treated the following day, as indicated, with interferon-gamma (IFNγ, Life Technologies, PHC4031) in the absence or presence of L-tryptophan (50 ug/ml in A549 cells and 33 ug/ml in TZM-bl cells) or 1-MT (100 ug/ml). The unit dose of IFNγ was determined using the most conservative estimate given by the manufacturer ($2x10^6$ units/mg). At 24h after IFNγ treatment, cells were infected with VSV-G pseudotyped NHG for 6h, after which the inoculum was removed, and cells were returned to their original medium (containing IFNγ and 1-MT or L-trp as specified). For the incoming infectivity assay, the A549 cells were harvested and fixed at 44h after infection, and the GFP+ cells were enumerated using flow cytometry. In the outgoing, viral production assay in A549/TZM-bl cells, at 44h post-infection cells were lysed in SDS sample buffer and the virus-containing supernatant was harvested and filtered and titrated onto MT4 cells as described above.

Single cycle infectivity assays conducted using GHOSTX4 and GHOSTX4 TRIM56 cells were executed by infecting cells at an MOI of 0.5 with VSV-pseudotyped HIV-1 NL4-3 or NL-YU2. Incoming virus was removed and replaced with fresh medium 16 hours post infection. Forty-eight hours post-infection the virions were harvested from culture supernatants and cells were lysed in SDS sample buffer.

Spreading viral replication assays

For HIV-1 spreading replication assays in transduced MT4 cells, these cells were doxycycline-treated or untreated for 24h and then were infected with HIV-1 (NHG) at a low MOI of ~0.01. Alternatively, MT4-LTR-GFP cells (and derivatives that were subjected to control or TRIM56 CRISPR knockout) were infected with NL4-3 at an MOI of 0.001 following either no treatment or treatment with 25U/ml IFNα for 24h. Infected GFP+ cells were enumerated every 1-2 days by using flow cytometry.

Spreading replication assays conducted in GHOSTX4-vector and GHOSTX4-TRIM56 clones were performed by infecting cells at an MOI of 0.01 with HIV-1 NL4-3 and derivatives (e.g. HIV-1(TRIM56R)). Every two or three days the cells were split 1 in 5 until cell death terminated the experiment. A portion of the cells was fixed in 2% paraformaldehyde (final concentration) and the level of infection was measured using GFP expression determined through flow cytometry.

Derivation of HIV-1/TRIM5R

To adapt HIV-1 to replicate in GHOSTX4#2 cells, HIV-1/NL4-3 that had been passaged twice in other GHOSTX4-TRIM56 clones was used to infect GHOSTX4 and GHOSTX4-TRIM56#2 cells and virus replication was monitored by enumerating GFP+ cells. When viral spread became evident in GHOSTX4-TRIM56#2 cells (>50% GFP+ cells) viral supernatant from GHOSTX4-TRIM56#2 cells was filtered and used to inoculate fresh cultures of GHOSTX4 and GHOSTX4-TRIM56#2 (MOI=0.01-0.02). After 8 passages in GHOSTX4-TRIM56#2 cells, a full length HIV-1 clone was derived from infected GHOSTX4-TRIM56#2 cells by extracting genomic DNA (Qiagen QIAamp DNA Mini Kit) from the cells when they were 50% GFP positive and amplifying the integrated viral DNA in two portions. The 5'half was amplified using HIV-1 specific primers from the 5'LTR to the *Eco*RI site in *vpr*, the 3' half was amplified using HIV-1 specific primers from the *Eco*RI site in *vpr* to the end of the 3'LTR. The amplified 5' and 3' portions of TRIM56R were then used to generate chimeric proviral plasmids containing portions of HIV-1/NL4-3 and HIV-1/TRIM56R.

Quantitative Western blot analyses

Cell lysates and virions (isolated via centrifugation through 20% sucrose) were resuspended in SDS sample buffer, resolved on NuPage 4-12% Bis-Tris gels (Novex), blotted onto nitrocellulose membranes (GE Healthcare), and probed with either anti-HIV p24 capsid antibody (183-H12-5C, NIH AIDS reagents program), anti-HIV-1 gp120 (American Research Products, 12-6205-1), anti-HIV-1 gp160 (NIH AIDS Reagents Program HIV-1 gp41 Hybridoma Chessie 8), anti-HIV-1 Nef (NIH AIDS Reagents Program, 2949) anti-tubulin (Sigma, T6074), anti-actin (JLA20 hybridoma, Developmental Studies Hybridoma Bank, University of Iowa), anti-c-myc (9E10 hybridoma, Developmental Studies Hybridoma Bank, University of Iowa), anti-TRIM56 (Abcam ab154862) and anti-IDO1 (Abcam, ab55305). Membranes were subsequently probed with secondary, fluorescently labeled goat anti-mouse/anti-rabbit antibodies labeled with IRDye® 800CW or IRDye® 680RD (LI-COR Biosciences or Thermo Scientific) and scanned using a Li-Cor Odyssey Scanner.

Microarray analyses

Total RNA was extracted, using the RNeasy Plus Mini kit (Qiagen), from MT4-LTR-GFP cells control subclones and CRISPR knockout subclones that were untreated or treated with 25 U/ml IFNα (Sigma) for 24 h before harvest.

Supplemental References

Adachi, A., Gendelman, H.E., Koenig, S., Folks, T., Willey, R., Rabson, A., and Martin, M.A. (1986). Production of acquired immunodeficiency syndrome-associated retrovirus in human and nonhuman cells transfected with an infectious molecular clone. Journal of virology *59*, 284-291.

Andrejeva, J., Childs, K.S., Young, D.F., Carlos, T.S., Stock, N., Goodbourn, S., and Randall, R.E. (2004). The V proteins of paramyxoviruses bind the IFN-inducible RNA helicase, mda-5, and inhibit its activation of the IFN-beta promoter. Proceedings of the National Academy of Sciences of the United States of America *101*, 17264-17269.

Berger, G., Durand, S., Fargier, G., Nguyen, X.N., Cordeil, S., Bouaziz, S., Muriaux, D., Darlix, J.L., and Cimarelli, A. (2011). APOBEC3A is a specific inhibitor of the early phases of HIV-1 infection in myeloid cells. PLoS pathogens *7*, e1002221.

Bock, M., Heinkelein, M., Lindemann, D., and Rethwilm, A. (1998). Cells expressing the human foamy virus (HFV) accessory Bet protein are resistant to productive HFV superinfection. Virology *250*, 194-204.

Brass, A.L., Huang, I.C., Benita, Y., John, S.P., Krishnan, M.N., Feeley, E.M., Ryan, B.J., Weyer, J.L., van der Weyden, L., Fikrig, E.*, et al.* (2009). The IFITM proteins mediate cellular resistance to influenza A H1N1 virus, West Nile virus, and dengue virus. Cell *139*, 1243-1254.

Bregnard, C., Zamborlini, A., Leduc, M., Chafey, P., Camoin, L., Saib, A., Benichou, S., Danos, O., and Basmaciogullari, S. (2013). Comparative proteomic analysis of HIV-1 particles reveals a role for Ezrin and EHD4 in the Nef-dependent increase of virus infectivity. Journal of virology *87*, 3729-3740.

Burdette, D.L., Monroe, K.M., Sotelo-Troha, K., Iwig, J.S., Eckert, B., Hyodo, M., Hayakawa, Y., and Vance, R.E. (2011). STING is a direct innate immune sensor of cyclic di-GMP. Nature *478*, 515-518.

Compton, A.A., Bruel, T., Porrot, F., Mallet, A., Sachse, M., Euvrard, M., Liang, C., Casartelli, N., and Schwartz, O. (2014). IFITM proteins incorporated into HIV-1 virions impair viral fusion and spread. Cell host & microbe *16*, 736-747.

Deb, A., Haque, S.J., Mogensen, T., Silverman, R.H., and Williams, B.R. (2001). RNA-dependent protein kinase PKR is required for activation of NF-kappa B by IFN-gamma in a STAT1-independent pathway. Journal of immunology *166*, 6170-6180.

Donahue, D.A., Amraoui, S., di Nunzio, F., Kieffer, C., Porrot, F., Opp, S., Diaz-Griffero, F., Casartelli, N., and Schwartz, O. (2016). SUN2 Overexpression Deforms Nuclear Shape and Inhibits HIV. Journal of virology *90*, 4199-4214.

Furtak, V., Mulky, A., Rawlings, S.A., Kozhaya, L., Lee, K., Kewalramani, V.N., and Unutmaz, D. (2010). Perturbation of the P-body component Mov10 inhibits HIV-1 infectivity. PloS one *5*, e9081.

Gao, D., Wu, J., Wu, Y.T., Du, F., Aroh, C., Yan, N., Sun, L., and Chen, Z.J. (2013). Cyclic GMP-AMP synthase is an innate immune sensor of HIV and other retroviruses. Science *341*, 903-906.

Gao, G., Guo, X., and Goff, S.P. (2002). Inhibition of retroviral RNA production by ZAP, a CCCH-type zinc finger protein. Science *297*, 1703-1706.

Gibbert, K., Francois, S., Sigmund, A.M., Harper, M.S., Barrett, B.S., Kirchning, C.J., Lu, M., Santiago, M.L., and Dittmer, U. (2014). Friend retrovirus drives cytotoxic effectors through Toll-like receptor 3. Retrovirology *11*, 126.

Goujon, C., Moncorge, O., Bauby, H., Doyle, T., Ward, C.C., Schaller, T., Hue, S., Barclay, W.S., Schulz, R., and Malim, M.H. (2013). Human MX2 is an interferon-induced post-entry inhibitor of HIV-1 infection. Nature *502*, 559-562.

Hatziioannou, T., Cowan, S., Goff, S.P., Bieniasz, P.D., and Towers, G.J. (2003). Restriction of multiple divergent retroviruses by Lv1 and Ref1. The EMBO journal *22*, 385-394.

Hishiki, T., Ohshima, T., Ego, T., and Shimotohno, K. (2007). BCL3 acts as a negative regulator of transcription from the human T-cell leukemia virus type 1 long terminal repeat through interactions with TORC3. The Journal of biological chemistry *282*, 28335-28343.

Kane, M., Case, L.K., Wang, C., Yurkovetskiy, L., Dikiy, S., and Golovkina, T.V. (2011). Innate immune sensing of retroviral infection via Toll-like receptor 7 occurs upon viral entry. Immunity *35*, 135-145.

Kemler, I., Barraza, R., and Poeschla, E.M. (2002). Mapping the encapsidation determinants of feline immunodeficiency virus. Journal of virology *76*, 11889-11903.

Kim, Y.M., Brinkmann, M.M., Paquet, M.E., and Ploegh, H.L. (2008). UNC93B1 delivers nucleotide-sensing toll-like receptors to endolysosomes. Nature *452*, 234-238.

Kuang, Z., Seo, E.J., and Leis, J. (2011). Mechanism of inhibition of retrovirus release from cells by interferon-induced gene ISG15. Journal of virology *85*, 7153-7161.

Lahaye, X., Satoh, T., Gentili, M., Cerboni, S., Silvin, A., Conrad, C., Ahmed-Belkacem, A., Rodriguez, E.C., Guichou, J.F., Bosquet, N., *et al.* (2016). Nuclear Envelope Protein SUN2 Promotes Cyclophilin-A-Dependent Steps of HIV Replication. Cell reports.
Lee, Y.N., and Bieniasz, P.D. (2007). Reconstitution of an infectious human endogenous retrovirus. PLoS pathogens *3*, e10.
Leiden, J.M., Wang, C.Y., Petryniak, B., Markovitz, D.M., Nabel, G.J., and Thompson, C.B. (1992). A novel Ets-related transcription factor, Elf-1, binds to human immunodeficiency virus type 2 regulatory elements that are required for inducible trans activation in T cells. Journal of virology *66*, 5890-5897.
Liu, Z., Pan, Q., Ding, S., Qian, J., Xu, F., Zhou, J., Cen, S., Guo, F., and Liang, C. (2013). The interferon-inducible MxB protein inhibits HIV-1 infection. Cell host & microbe *14*, 398-410.
Lu, J., Pan, Q., Rong, L., He, W., Liu, S.L., and Liang, C. (2011). The IFITM proteins inhibit HIV-1 infection. Journal of virology *85*, 2126-2137.
Matsuura, A., Tsukada, J., Mizobe, T., Higashi, T., Mouri, F., Tanikawa, R., Yamauchi, A., Hirashima, M., and Tanaka, Y. (2009). Intracellular galectin-9 activates inflammatory cytokines in monocytes. Genes to cells : devoted to molecular & cellular mechanisms *14*, 511-521.
McLaren, P.J., Gawanbacht, A., Pyndiah, N., Krapp, C., Hotter, D., Kluge, S.F., Gotz, N., Heilmann, J., Mack, K., Sauter, D., *et al.* (2015). Identification of potential HIV restriction factors by combining evolutionary genomic signatures with functional analyses. Retrovirology *12*, 41.
Mitrophanous, K., Yoon, S., Rohll, J., Patil, D., Wilkes, F., Kim, V., Kingsman, S., Kingsman, A., and Mazarakis, N. (1999). Stable gene transfer to the nervous system using a non-primate lentiviral vector. Gene therapy *6*, 1808-1818.
Nakamura, N., Lill, J.R., Phung, Q., Jiang, Z., Bakalarski, C., de Maziere, A., Klumperman, J., Schlatter, M., Delamarre, L., and Mellman, I. (2014). Endosomes are specialized platforms for bacterial sensing and NOD2 signalling. Nature *509*, 240-244.
Neil, S., Martin, F., Ikeda, Y., and Collins, M. (2001). Postentry restriction to human immunodeficiency virus-based vector transduction in human monocytes. Journal of virology *75*, 5448-5456.
Neil, S.J., Zang, T., and Bieniasz, P.D. (2008). Tetherin inhibits retrovirus release and is antagonized by HIV-1 Vpu. Nature *451*, 425-430.
Newman, R.M., Hall, L., Connole, M., Chen, G.L., Sato, S., Yuste, E., Diehl, W., Hunter, E., Kaur, A., Miller, G.M., *et al.* (2006). Balancing selection and the evolution of functional polymorphism in Old World monkey TRIM5alpha. Proceedings of the National Academy of Sciences of the United States of America *103*, 19134-19139.
Nguyen, D.G., Wolff, K.C., Yin, H., Caldwell, J.S., and Kuhen, K.L. (2006). "UnPAKing" human immunodeficiency virus (HIV) replication: using small interfering RNA screening to identify novel cofactors and elucidate the role of group I PAKs in HIV infection. Journal of virology *80*, 130-137.
Pasare, C., and Medzhitov, R. (2005). Toll-like receptors: linking innate and adaptive immunity. Advances in experimental medicine and biology *560*, 11-18.
Pauls, E., Ruiz, A., Riveira-Munoz, E., Permanyer, M., Badia, R., Clotet, B., Keppler, O.T., Ballana, E., and Este, J.A. (2014). p21 regulates the HIV-1 restriction factor SAMHD1. Proceedings of the National Academy of Sciences of the United States of America *111*, E1322-1324.
Perez-Caballero, D., Soll, S.J., and Bieniasz, P.D. (2008). Evidence for restriction of ancient primate gammaretroviruses by APOBEC3 but not TRIM5alpha proteins. PLoS pathogens *4*, e1000181.
Pincetic, A., Kuang, Z., Seo, E.J., and Leis, J. (2010). The interferon-induced gene ISG15 blocks retrovirus release from cells late in the budding process. Journal of virology *84*, 4725-4736.
Randall, R.E., and Goodbourn, S. (2008). Interferons and viruses: an interplay between induction, signalling, antiviral responses and virus countermeasures. The Journal of general virology *89*, 1-47.
Sayah, D.M., Sokolskaja, E., Berthoux, L., and Luban, J. (2004). Cyclophilin A retrotransposition into TRIM5 explains owl monkey resistance to HIV-1. Nature *430*, 569-573.
Schmidt, M., and Rethwilm, A. (1995). Replicating foamy virus-based vectors directing high level expression of foreign genes. Virology *210*, 167-178.
Sheehy, A.M., Gaddis, N.C., Choi, J.D., and Malim, M.H. (2002). Isolation of a human gene that inhibits HIV-1 infection and is suppressed by the viral Vif protein. Nature *418*, 646-650.
Soll, S.J., Neil, S.J., and Bieniasz, P.D. (2010). Identification of a receptor for an extinct virus. Proceedings of the National Academy of Sciences of the United States of America *107*, 19496-19501.
Soneoka, Y., Cannon, P.M., Ramsdale, E.E., Griffiths, J.C., Romano, G., Kingsman, S.M., and Kingsman, A.J. (1995). A transient three-plasmid expression system for the production of high titer retroviral vectors. Nucleic acids research *23*, 628-633.

Stremlau, M., Owens, C.M., Perron, M.J., Kiessling, M., Autissier, P., and Sodroski, J. (2004). The cytoplasmic body component TRIM5alpha restricts HIV-1 infection in Old World monkeys. Nature *427*, 848-853.
Taylor, H.E., Khatua, A.K., and Popik, W. (2014). The innate immune factor apolipoprotein L1 restricts HIV-1 infection. Journal of virology *88*, 592-603.
Telenti, A., and Johnson, W.E. (2012). Host genes important to HIV replication and evolution. Cold Spring Harbor perspectives in medicine *2*, a007203.
Wang, X., Han, Y., Dang, Y., Fu, W., Zhou, T., Ptak, R.G., and Zheng, Y.H. (2010). Moloney leukemia virus 10 (MOV10) protein inhibits retrovirus replication. The Journal of biological chemistry *285*, 14346-14355.
Wiegand, H.L., Doehle, B.P., Bogerd, H.P., and Cullen, B.R. (2004). A second human antiretroviral factor, APOBEC3F, is suppressed by the HIV-1 and HIV-2 Vif proteins. The EMBO journal *23*, 2451-2458.
Wilson, S.J., Schoggins, J.W., Zang, T., Kutluay, S.B., Jouvenet, N., Alim, M.A., Bitzegeio, J., Rice, C.M., and Bieniasz, P.D. (2012). Inhibition of HIV-1 particle assembly by 2',3'-cyclic-nucleotide 3'-phosphodiesterase. Cell host & microbe *12*, 585-597.
Wilson, S.J., Webb, B.L., Ylinen, L.M., Verschoor, E., Heeney, J.L., and Towers, G.J. (2008). Independent evolution of an antiviral TRIMCyp in rhesus macaques. Proceedings of the National Academy of Sciences of the United States of America *105*, 3557-3562.
Xu, H., Yang, J., Gao, W., Li, L., Li, P., Zhang, L., Gong, Y.N., Peng, X., Xi, J.J., Chen, S.*, et al.* (2014). Innate immune sensing of bacterial modifications of Rho GTPases by the Pyrin inflammasome. Nature *513*, 237-241.
Yan, N., Regalado-Magdos, A.D., Stiggelbout, B., Lee-Kirsch, M.A., and Lieberman, J. (2010). The cytosolic exonuclease TREX1 inhibits the innate immune response to human immunodeficiency virus type 1. Nature immunology *11*, 1005-1013.
Yoon, C.H., Kim, S.Y., Byeon, S.E., Jeong, Y., Lee, J., Kim, K.P., Park, J., and Bae, Y.S. (2015). p53-derived host restriction of HIV-1 replication by protein kinase R-mediated Tat phosphorylation and inactivation. Journal of virology *89*, 4262-4280.
Yu, Q., Chen, D., Konig, R., Mariani, R., Unutmaz, D., and Landau, N.R. (2004). APOBEC3B and APOBEC3C are potent inhibitors of simian immunodeficiency virus replication. The Journal of biological chemistry *279*, 53379-53386.
Zennou, V., and Bieniasz, P.D. (2006). Comparative analysis of the antiretroviral activity of APOBEC3G and APOBEC3F from primates. Virology *349*, 31-40.
Zhang, F., Hatziioannou, T., Perez-Caballero, D., Derse, D., and Bieniasz, P.D. (2006). Antiretroviral potential of human tripartite motif-5 and related proteins. Virology *353*, 396-409.